HIGH POWER MICROWAVES: APPLICATIONS AND DEVICES FOR THEIR GENERATION AND AMPLIFICATION

B. N. Basu

bnbasu_bhu@rediffmail.com

Centre of Research in Microwave Tubes
Department of Electronics Engineering
Institute of Technology
Banaras Hindu University
Varanasi

Part 2

Military use of high power microwave energy

HPM electronic warfare

DEW

EMP coupling Mechanisms

High energy lasers (HEL)

Charged particle beam (CPB)

Neutral particle beam (NPB)

High Power Microwaves (HPM)

Breakdown voltage ratings of electronic devices

Upset levels for electronic devices

Electronic device burnout thresholds

Microwave bomb or Electromagnetic bomb (E-bomb) for EMP

MHD generator

Flux compression generator FCG

E-bomb warhead using FCG and vircator

SSD versus microwave tube

HPM system configuration

Technology gap in the millimeter-wave frequency range

Trends in microwave tubes: improved performance conventional, MPM and micro-fabricated, IREB-driven, and fast-wave tubes

HPM cathodes

MBK

Vircator

BWO Reltron

MILO

Orotron or RDG

MWCG

MWDG

Pasotron

Microwave Tubes

SSD versus VED/ Microwave Tube

Issue	SSD	VED/ Microwave tube
Collisional heat produced by electron stream	Throughout volume	At the collector
Operating temperature	Lower temperature operation for a longer life (lower mobility — a greater drag or inertial forces due to collision) Degradation at a higher temperature due to dopant migrating excessively, lattice becoming imperfect, mobility getting reduced impairing high frequency performance Wide-band-gap semiconductors like SiC and GaN to be used for high temperature operation	Higher temperature operation

SSD versus VED/ Microwave Tube (*continued*)

Issue	SSD	VED/ Microwave tube
Breakdown limit on maximum electric field inside the device	Lower	Higher
Base plate size Determined by cooling efficiency increasing with (i) the temperature difference between the hot surface and the cool environment and (ii) the surface area of the hot surface	Larger	Smaller (higher collector temperature)
Peak pulsed power	Lower Calls for power combining by multiple transistors and proportionate increase in package size	Higher Beam may be pulsed in the region separated from the interaction region
Ultra-bandwidth performance (Three-plus-octaves)	Possible below 1 GHz Corresponding to longer wavelengths ensuring negligible phase difference, for instance, in the voltage between the emitter and base	Usually not possible Controlling the structure dispersion is a challenging problem

Difficulty of replacing VEDs/ Microwave Tubes by SSDs

Examples:

(i) Satellite qualified devices requiring 5 million hour MTBF

SSDs tried out between 1990 and 1998 (for instance, 50% TWTs and 50% SSDs in 1995)

SSDs declined in 1998 and beyond (90% TWTs and 10% SSDs)

Issues: Ionisation radiation, Cooling via radiation is strongly preferred (no air in space for convection cooling, and refrigerants are luxury)

SSDs, with no high temperature components, have a less potential for efficient cooling requiring large base plate sizes.

SSDs are radiation degradable

VEDs/ Microwave tubes are preferred

(ii) Towed decoys (small pods containing ECM transmitters that are dragged at high speeds behind a fighter jet)

Issues: high temperature of the decoy due to air friction and high power operation of ECM transmitters

VEDs/ Microwave tubes are preferred

Classification of Microwave Tubes

(***Basis of classification is the mechanism of electron beam bunching and conversion of beam energy into electromagnetic energy***)

- O- and M-types (O standing for TPO — tubes à propagation des ondes, and M for TPOM — tubes à propagation des ondes à champs magnetique)
- Kinetic energy and potential energy conversion types
- Longitudinal space-charge-wave, transverse space-charge-wave, and cyclotron-mode interaction types
- Distributed and localised interaction types
- Slow-wave and fast-wave types
- Non-relativistic and relativistic bunching types
- Cerenkov, transition, and bremsstrahlung radiation types
- CRM instability and Weibel instability types

MAGIC MOVIE

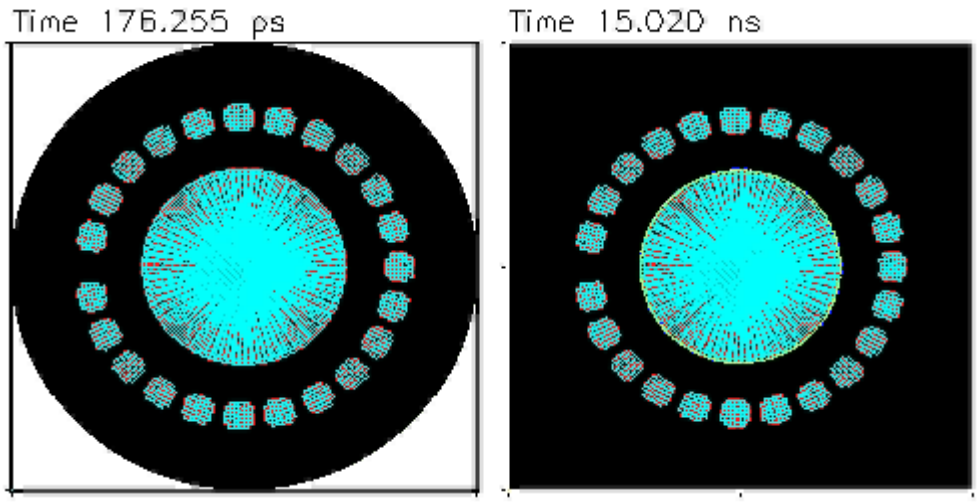

Magnetron

Cerenkov radiation type is characterised by electrons moving in a medium with a speed greater than the phase velocity of electromagnetic waves in the medium

(TWT, BWO)

Transition radiation type is characterised by electrons passing through the boundary between two media with different refractive indices or passing through perturbations in a medium such as conducting grids and a gap between conducting surfaces

(Klystron)

Bremsstrahlung radiation type is characterised by electrons accelerating or decelerating in an electric or magnetic field

(Gyrotron, VIRCATOR)

Maximum power (P) limitation of a conventional microwave tube follows the frequency (f) dependence:

$$P = \frac{\text{constant}}{f^{m}}$$

where m is determined by the various limiting factors as follows:

m	Limiting factor
1-2	Thermal dissipation
2.5	RF losses
4.5	Current density, RF losses, thermal dissipation
4.5-5.5	CW devices
3	Pulsed devices if the average power is unimportant

Technology gap
in the millimeter-wave frequency range

Increase of the operating frequencies of conventional microwave tubes to millimeter waves by reducing critical dimensions

Power-limited by dc power dissipation, RF losses, attainable electron current density, beam confinement, heat transfer (restricting average power capability), material breakdown (arcing) (restricting peak power capability), technology limit in fabricating tiny parts, etc.

Decrease of the operating frequencies of quantum optical devices, like lasers

Reduction of the energy of each quantum

Difficulty in sustaining population inversion

Gyro-devices (fast-wave microwave tubes) to fill up the technology gap

CRM-instability-based devices: gyrotron, gyro-TWT, gyro-klystron (all fast-wave), Weibel-instability-based device: SWCA (slow-wave cyclotron amplifier), CRM-and-Weibel-instability-based device: CARM (cyclotron auto-resonance maser)

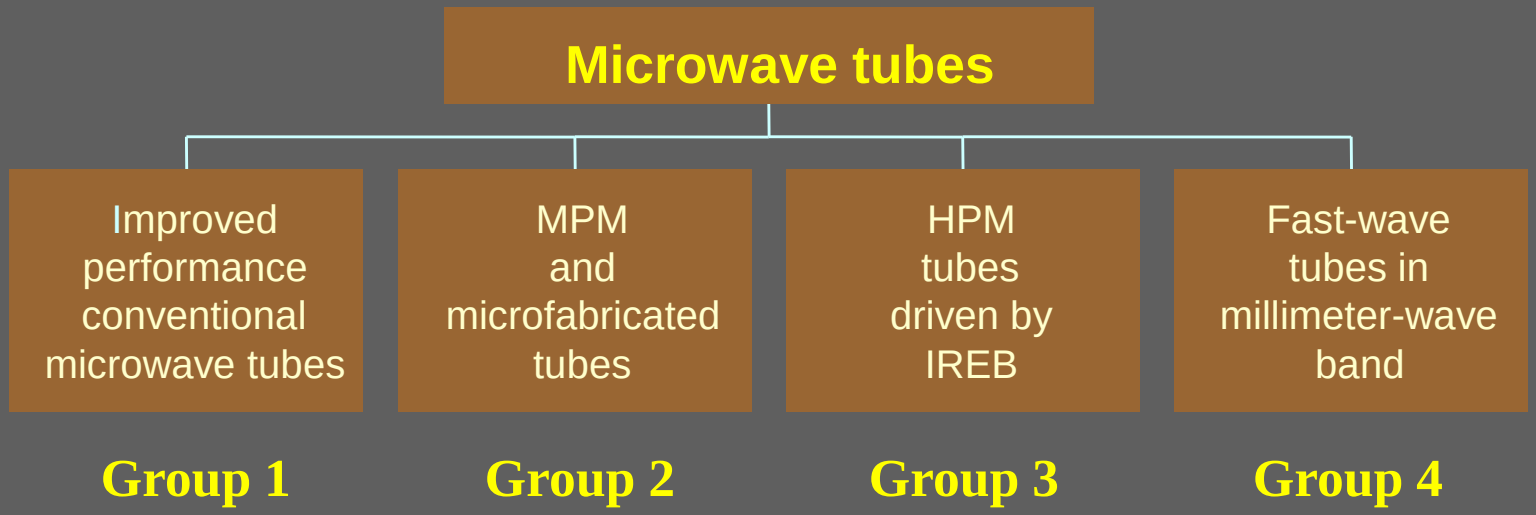
Microwave tubes
Improved performance conventional microwave tubes
MPM and microfabricated tubes
HPM tubes driven by IREB
Fast-wave tubes in millimeter-wave band
Group 1
Group 2
Group 3
Group 4

Grouping of microwave tubes (*continued*)

Group 1 Improved performance conventional microwave tubes: TWT (ultra-wide bandwidths, high efficiency); Klystron (EIK— wider bandwidths, higher power, EIO — millimeter-wave, low-power, MBK (large beam current, low beam voltage, high power, compact); Magnetron (oven, millimeter wave radar, relativistic — high power, long pulse).

Group 2 MPM and microfabricated tubes: MPM (ground and air-borne platforms, ECM and towed decoys, phased-array and power-combined EW, mobile and satellite communication, missile seeker and surveillance radar); Microfabricated tubes: Triode, Klystron, Klystrino, FW-TWT (folded waveguide TWT), etc.

Grouping of microwave tubes (*continued*)

Group 3 HPM Tube driven by IREB: VIRCATOR (no magnetic fields), BWO, Orotron (RDG), MWCG (multi-wave Cerenkov generator), MWDG (multi-wave diffraction generator), MILO (magnetically insulated line oscillator (no external magnetic field, magnetic insulation), Relativistic klystron, RELTRON, plasma-filled BWO, PASOTRON (plasma filled), etc.

Group 4 Fast-wave Tubes in millimeter-wave band: Gyrotron (High-harmonic (low magnetic fields), Large-orbit, Vane-loaded, Coaxial-cavity, Quasi-optical gyrotrons, Gyro-TWT (dielectric-loaded, disc-loaded), Frequency multiplying gyro-TWT, Gyro-klystron, Gyro-twystron, PHIGTRON (phase-coherent, harmonic multiplying, inverted gyro-twystron), Gyro-BWO, CARM, Peniotron, etc.

Group 1 of microwave tubes

Space TWT frequency band for telecommunication, TTC and radar (Group 1)

Telecommunication
Tracking, Telemetry, and Command (TTC)
Radar

Telecommunication

[50-200 W per TWT up to ~50 including redundant]
Space-to-earth
2.45-2.65 GHz (Mobile, fixed and broadcasting services)
3.4-4.8 GHz (Fixed services)
10.7-12.75 GHz (Fixed and broadcasting services)
37.5-43.5 GHz (Mobile, fixed and broadcasting services)
Space-to-space
22.5-23.5 GHz (Intersatellite)
32-33 GHz (Intersatellite)
59-71 GHz (Intersatellite)

Telecommunication

[50-200 W per TWT up to ~50 including redundant]

Space-to-earth

2.45-2.65 GHz (Mobile, fixed and broadcasting services)
3.4-4.8 GHz (Fixed services)
10.7-12.75 GHz (Fixed and broadcasting services)
37.5-43.5 GHz (Mobile, fixed and broadcasting services)

Space-to-space

22.5-23.5 GHz (Intersatellite)
32-33 GHz (Intersatellite)
59-71 GHz (Intersatellite)

Tracking, Telemetry, and Command (TTC)

[10-150 W per TWT (saturated CW) up to 8 including redundant]
2.2-2.3 GHz (Space operation, space research)
8.0-8.4 GHz (Earth exploration)
8.4-8.5 GHz (Space research)
25.5-27.0 GHz (Earth exploration)
31-32 GHz (Space research)
37-38 GHz (Space research)

Wideband multi-octave TWTs (Group 1)

Zero-to-slightly-negative-dispersion structure for wideband performance:

- Negative dispersion ensures the constancy of Pirece's velocity synchronisation parameter ***b***
- Anisotropically loaded helix:
  - Metal vane/ segment loaded envelope
- Inhomogeneously loaded helix:
  - Helix with tapered geometry dielectric supports such as half-moon-shaped and T-shaped supports

Multi-dispersion, multi-section helix for wideband performance:

- The value of ***N*** in the gain parameter ***CN*** depends on both the frequency and the interaction helix length.

- One positive-dispersion helix section of length l_1 is synchronous only at lower frequencies and the other no-dispersion helix section of length l_2 is synchronous both at lower and higher frequencies.

- Causes an increase in effective length to $l_1 + l_2$ at lower frequencies and a decrease in effective length to l_2 at higher frequencies
- Reduction of length at higher frequencies prevents oscillation at higher frequencies

MBK — multi-beam klystron (Group 1)

A parallel arrangement of low-perveance beamlets within a common RF structure for

- Large beam current and RF output power
- Low beam voltage and compactness due to reduced plasma wavelength (= beam velocity/ plasma frequency)
- PPM-stacked device

Each beam propagates in its own channel and then interacts with the field of a common interaction structure.

The space-charge effects and correspondingly the efficiency are the same as that of a single-beam tube but the beam current, beam perveance and power increase with the number of beamlets.

Typical SLAC MBK

- 10 individual 500 kV, 500 A (1.5 microperv) beams
- Output: 1 GW, 1 μs, 1.5 GHz, 36 dB gain, 40% efficiency

Typical L-3 Communications Electron Devices MBK

- 10 individual 115 kV, 13 A (1.6 microperv) beams
- Output: 10 MW, 1.5 μs, 1.3 GHz, 47 dB gain, 70% efficiency

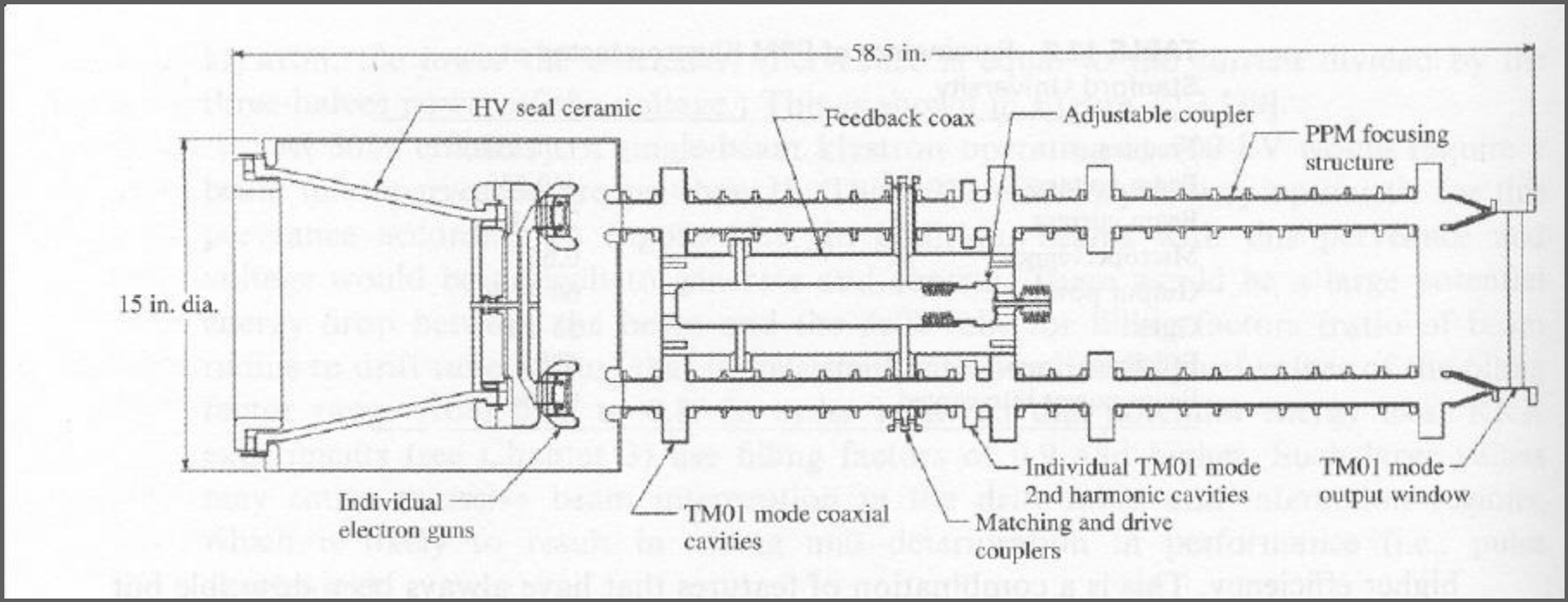
58.5 in.
HV seal ceramic
Feedback coax
Adjustable coupler
PPM focusing structure
15 in. dia.
Individual electron guns
TM01 mode coaxial cavities
Matching and drive couplers
Individual TM01 mode 2nd harmonic cavities
TM01 mode output window

10-beam MBK

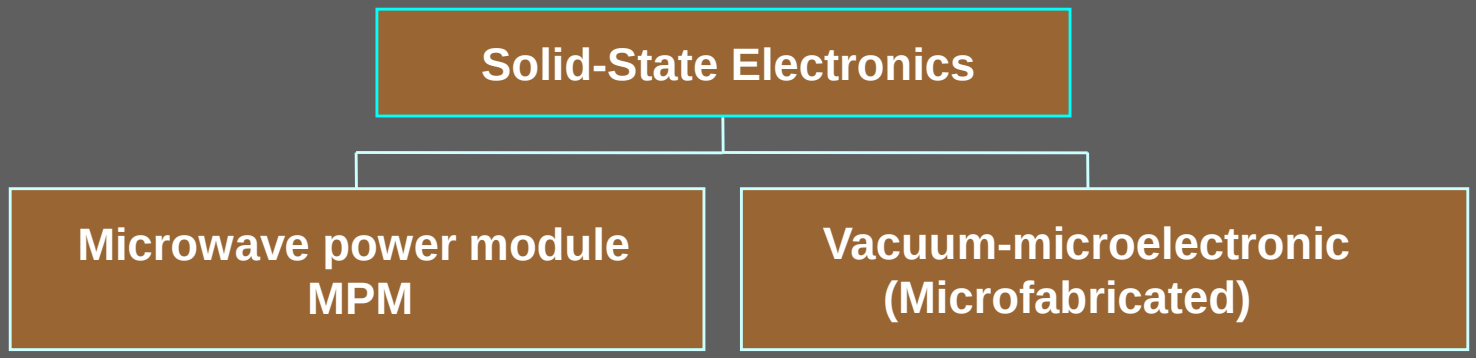

MPM Capitalizes relative strengths of both the solid-state and vacuum-electronic technologies

Utilises miniature, high-efficiency electronic power conditioner (EPC) technology to build a compact power amplifier

Vacuum-microelectronic (microfabricated) tube

Fundamental advantages: (i) electron velocity in vacuum about a thousand times grater than that in semiconductor solids, and higher signal processing speeds, (ii) less collisions of moving electrons with atoms and less associated energy loss as heat, (iii) precision imensioning of parts/ electromagnetic structures in the millimeter-wave and terahertz regimes, (iv) cold field-emission arrays cathodes (such as carbon nanotubes), etc.

MPM (Group 2)

Low cost high efficiency alternative to solid-state T/R modules conceived by US DoD's Advisory Group on Electron Devices in 1988

Synergistic combination of solid-state and vacuum-electronics

Gain sharing between SSA and TWT (Approx : 50:50)

Integration of SSA TWT and EPC into a Single Package

High Gain and High Output Power

High Efficiency

Wide Bandwidth

High Reliability

Low Noise Figure

Low cost, small size and light weight

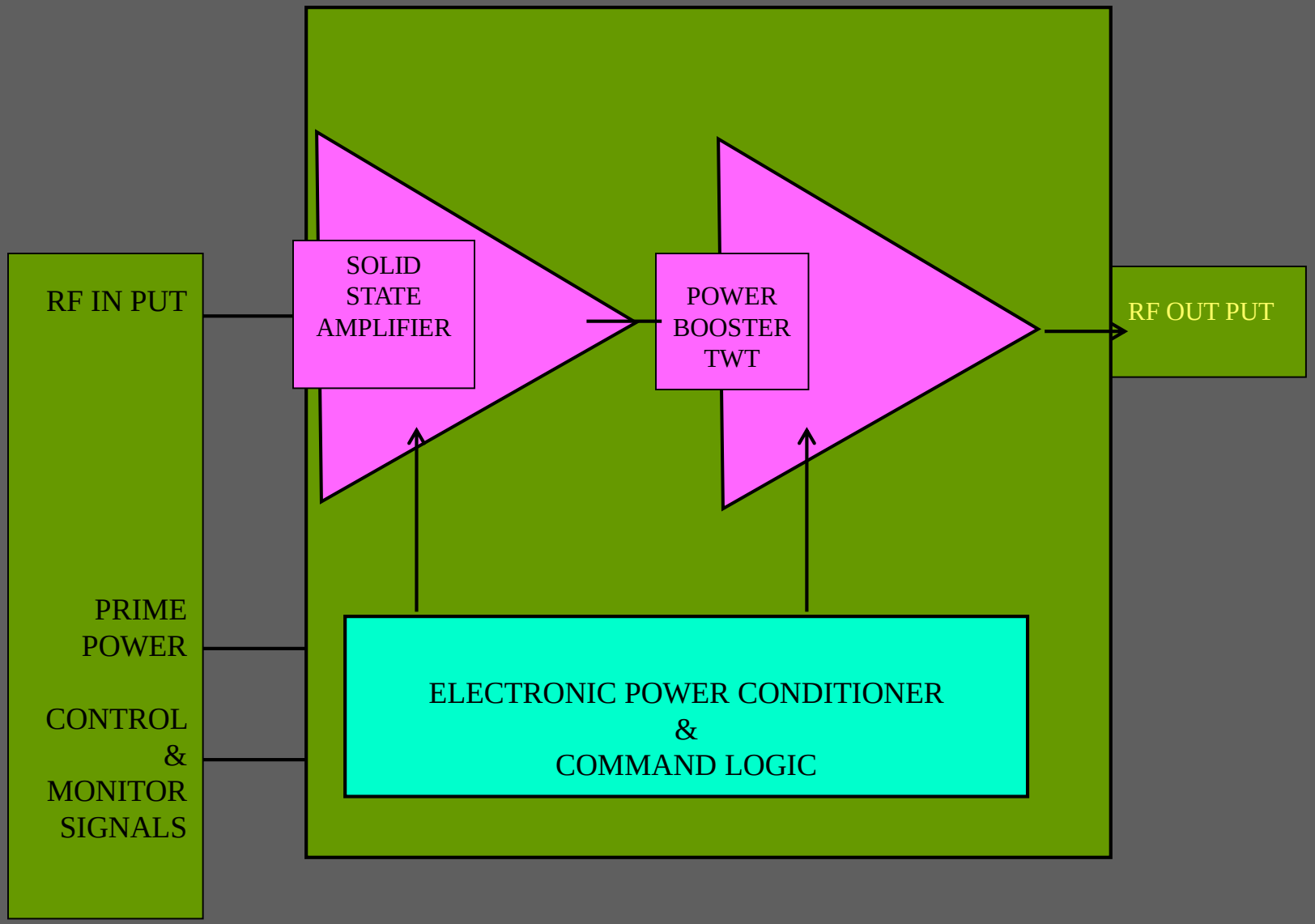

Microwave Power Module

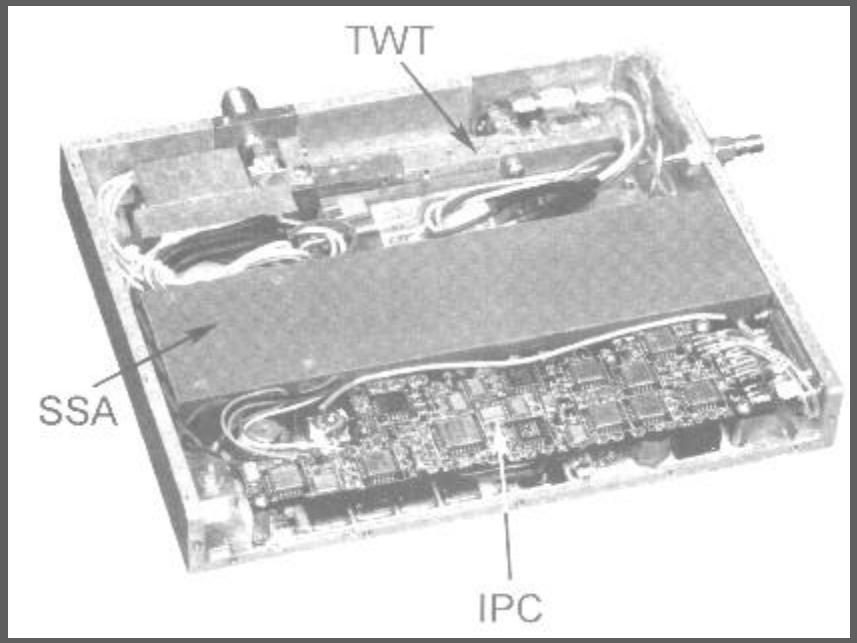

An 80-W, 6- to 8-GHz wideband MPM

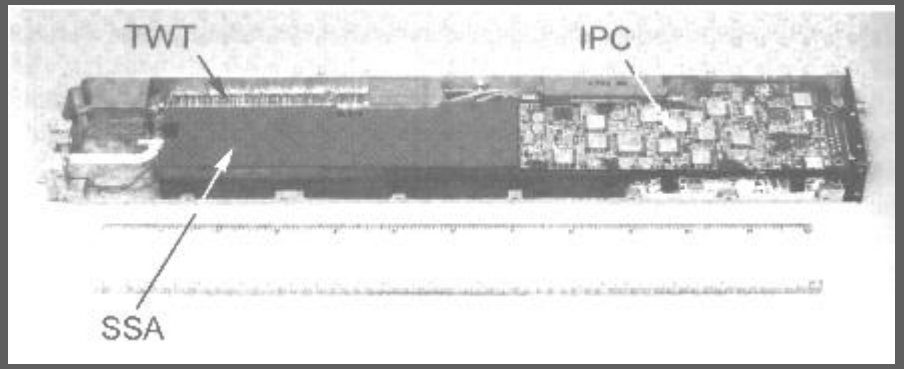

Ka-band MPM

Typical MPM parameters and features

2 to 46 GHz range

200 W CW, 2 Octaves, <7dB NF

Input drive: -100 dBm to 0 dBm

EPC: High density surface mount with compact planar transformers and high efficiency, high frequency SMPS

Prime power inputs: 270 V DC, 28 V DC, 115/230 V AC

Size and Weight: 40 $inch^3$ and 4 lb (100 W MPM)

Reliability: 15,000 hrs

Low voltage operation of the TWT booster: 5 kV (microwave) and 8 kV (mm wave)

Futuristic MPM

200 W MPM for high data-rate communication and EW; low-noise pulsed (400 W- 1kW) MPM for radar; millimeter-wave MPMs

(50 W broadband, 100 W narrow-band) for data links, satellite communication, image radar, towed decoys, ECM.

Looking forward to the inclusion of FEA, fast-turn-on cathode for ultra-miniature MPM, for new and exciting radar and communication

Vacuum microelectronic tubes (Group 2)

Typical Calabazas Creek TWTs

Folded waveguide slow-wave structure using microfabrication techniques like

EDM — electric discharge machining
DRIE — deep reactive ion etching
LIGA — lithographie, galvanoformung, abformung

Example: A folded (serpentine) trench is etched in silicon with a DRIE tool, and then gold-plated. Two such trenches bonded together form a folded waveguide
Field emission array cathode

LIGA (Group 2)

A typical microfabrication technique —

LIGA (lithographie, galvanoformung, abformung)

X-ray lithography using electroplating

A combination of deep-etch X-ray lithography and electroforming

Fabrication of vertical dimension from hundreds of microns to millimeters and horizontal dimension as small as microns for high frequency precision components

Multiple and identical batch production with a high yield
Reduced price

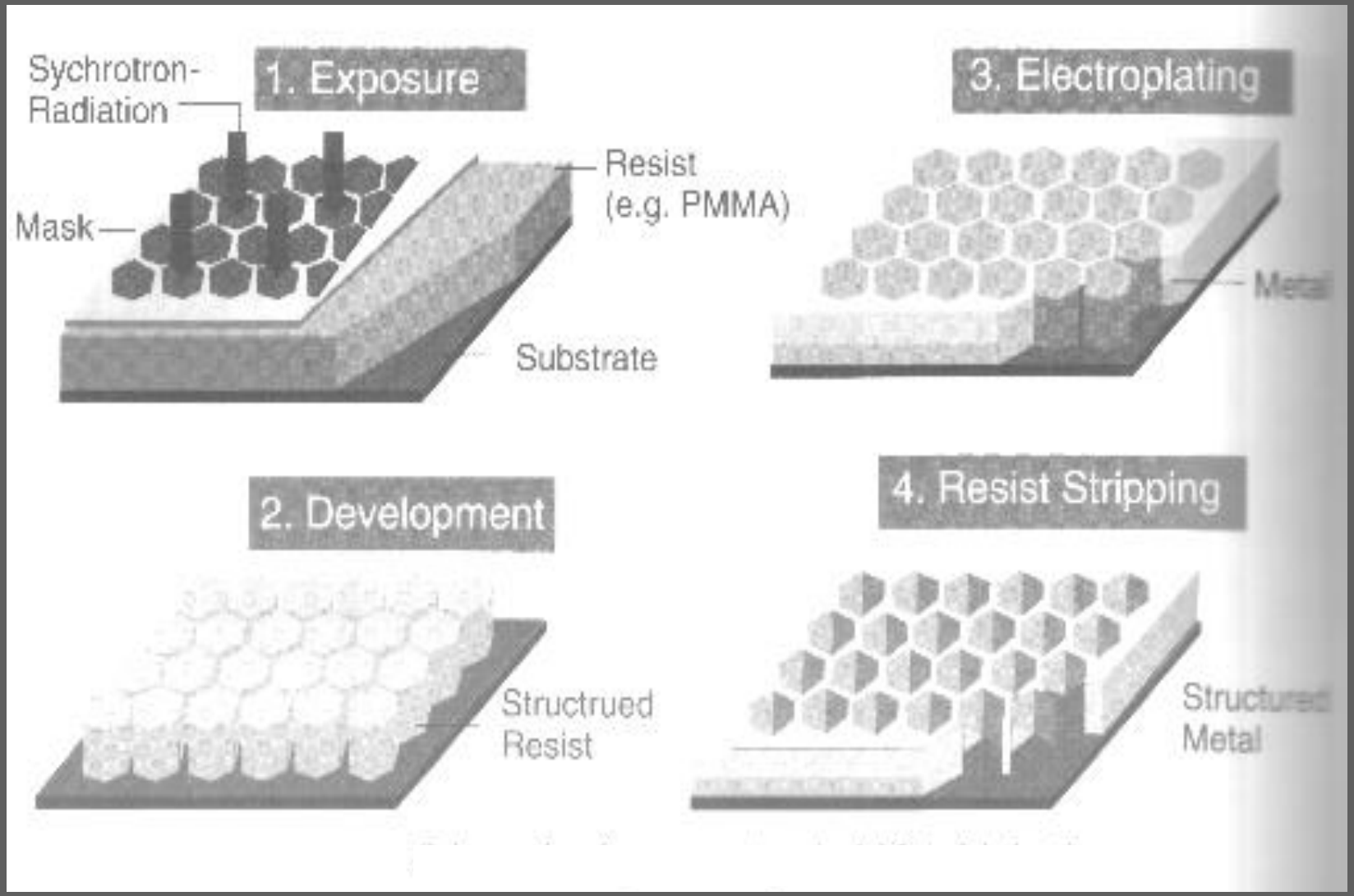

Schematic of process steps in LIGA fabrication

Gold-plated chrome mask

Polymethyl metahacrylate resist

Aluminum substrate (low atomic number to reduce back scattering)

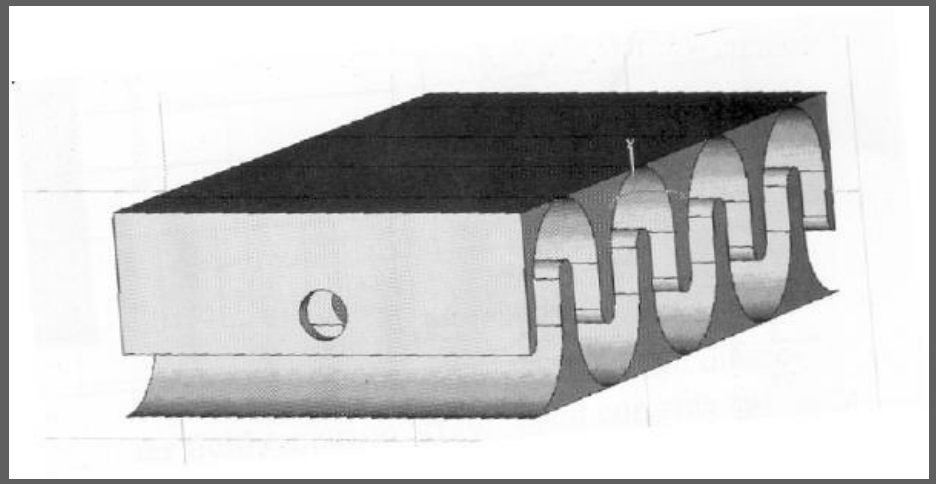

Folded waveguide for a TWT

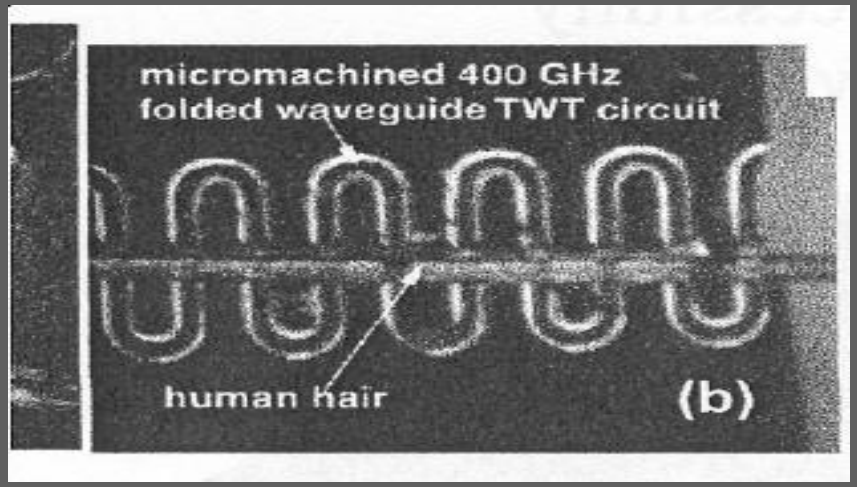

Vacuum microelectronic TWT on Chip (Group 2)

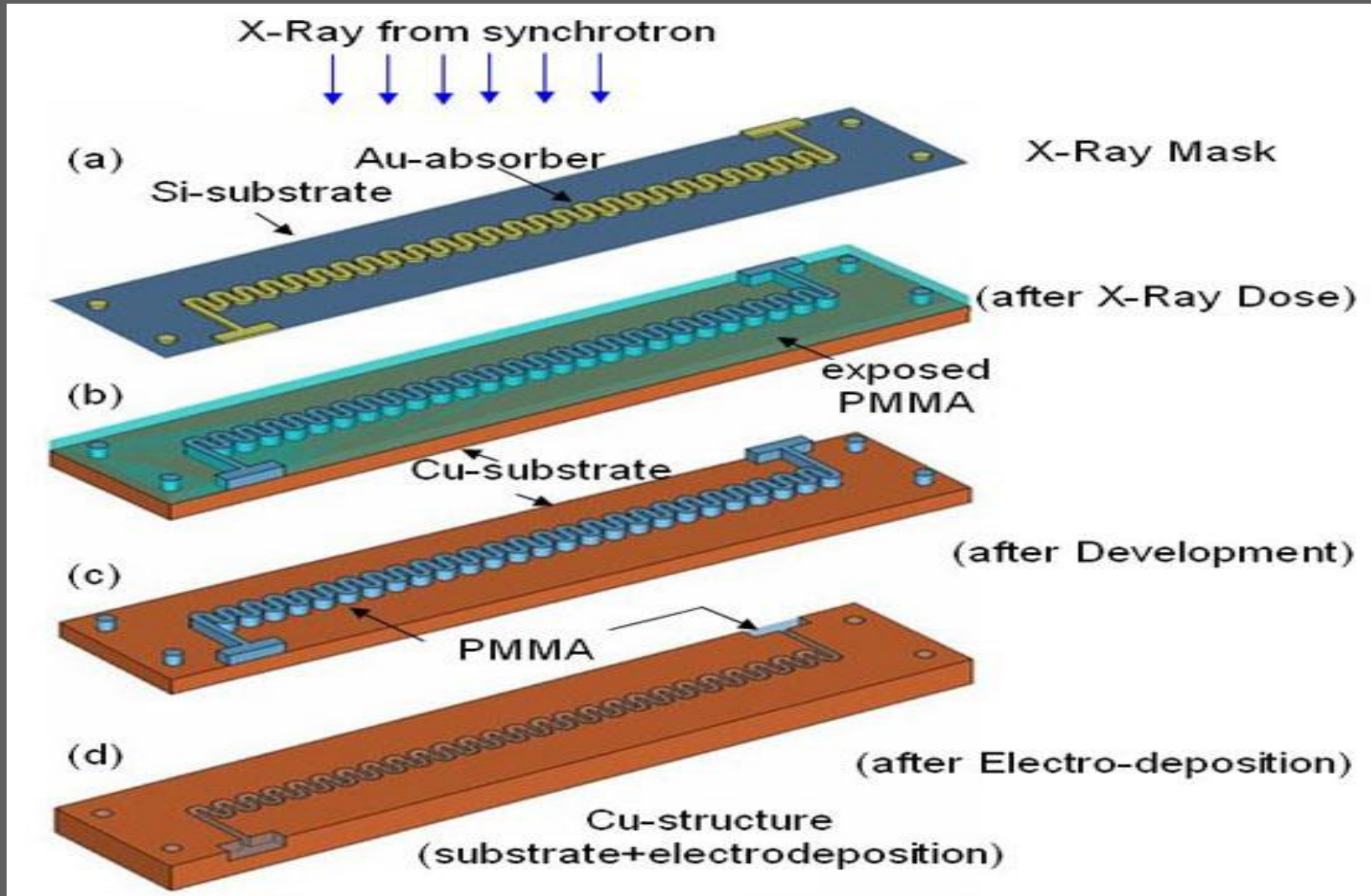

Typical parameters FW-TWT

83 GHz, 100 W; 12.8 kV, 0.156 A; 5% efficiency

180 GHz, 5 W; 12.8 kV, 0.013 A; 3% efficiency

Looking forward to the employment of nanotubes-FEA cathode (already implemented, for instance, in vacuum microelectronics triodes at the University of California)

Applications and suitability of microfabricated FW-TWT:

Space mission using micro-satellite clusters (in-space and terrestrial links)

Ideal for integration into network-centric military platforms

Suitable for communication transmitters networking diverse and widespread command posts, sensors and shooters

Suitable for compact amplifier technology as in Inverse SAR

Useful for maritime surveillance (where swaying of ships at sea allows precise identification from known superstructure)

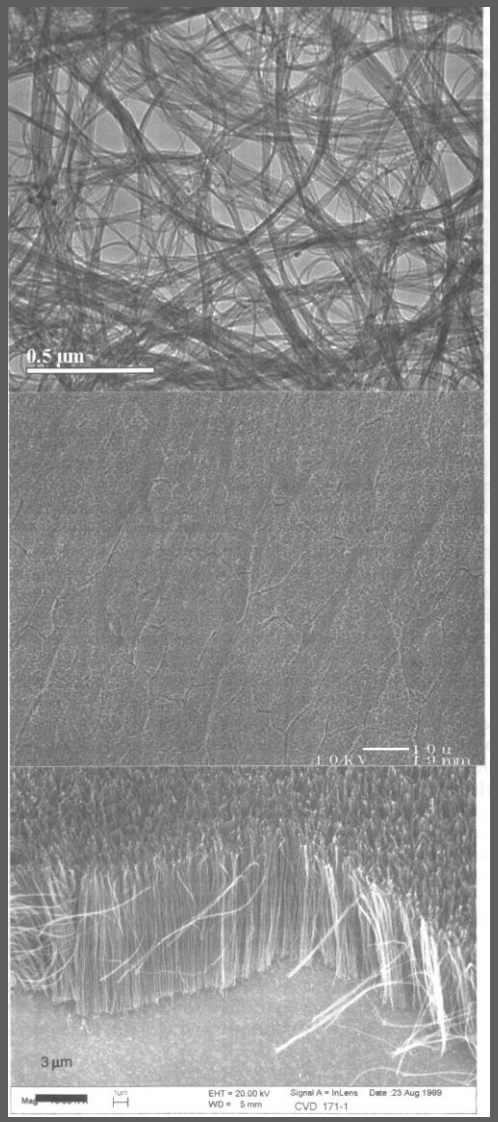

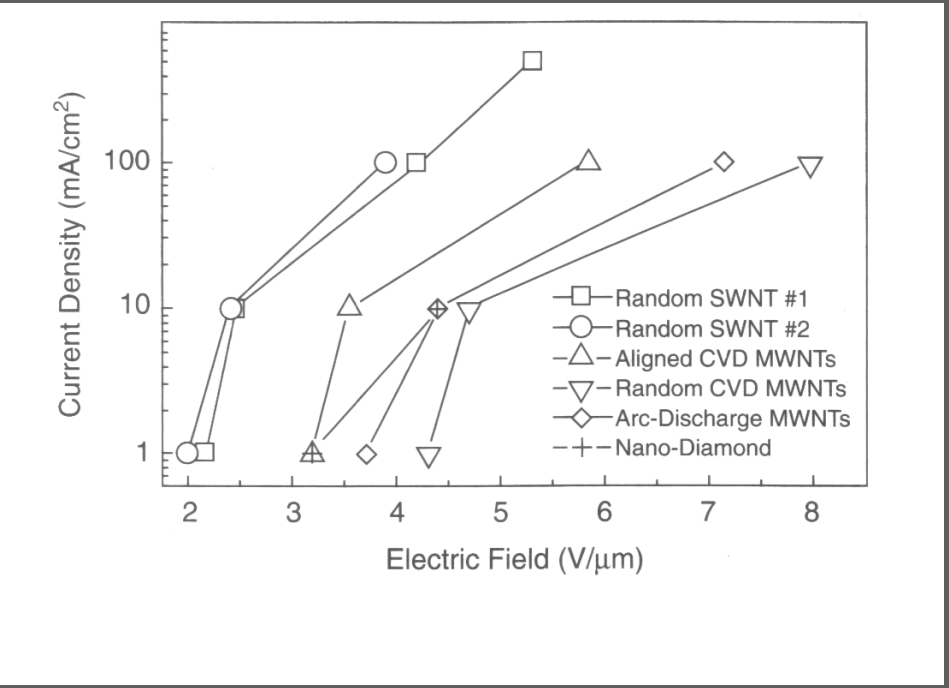

CNT emitters

Vacuum microelectronic klystrino (Group 2)

W band (~3 mm wavelength) Klystrinos in a klystron module
Dimensioning of conventional klystrons difficult in the millimeter-wave band
Lightweight PPM focusing possible in a klystrino
LIGA microfabrication technique for W-band klystrino cavity features with 2-3 μm tolerances and excellent surface finish

A typical klystron module, with 6 klystrinos in parallel, has separate electron guns 0.6 microperv each, cavities and PPM stacks, but a common vacuum and beam dump
Typical W-band klystrino parameters: 120 kV, 15 A; 0.5 MW peak, and 5 kW average; 6 inch dia, 12 inch length, < 20 lbs weight.

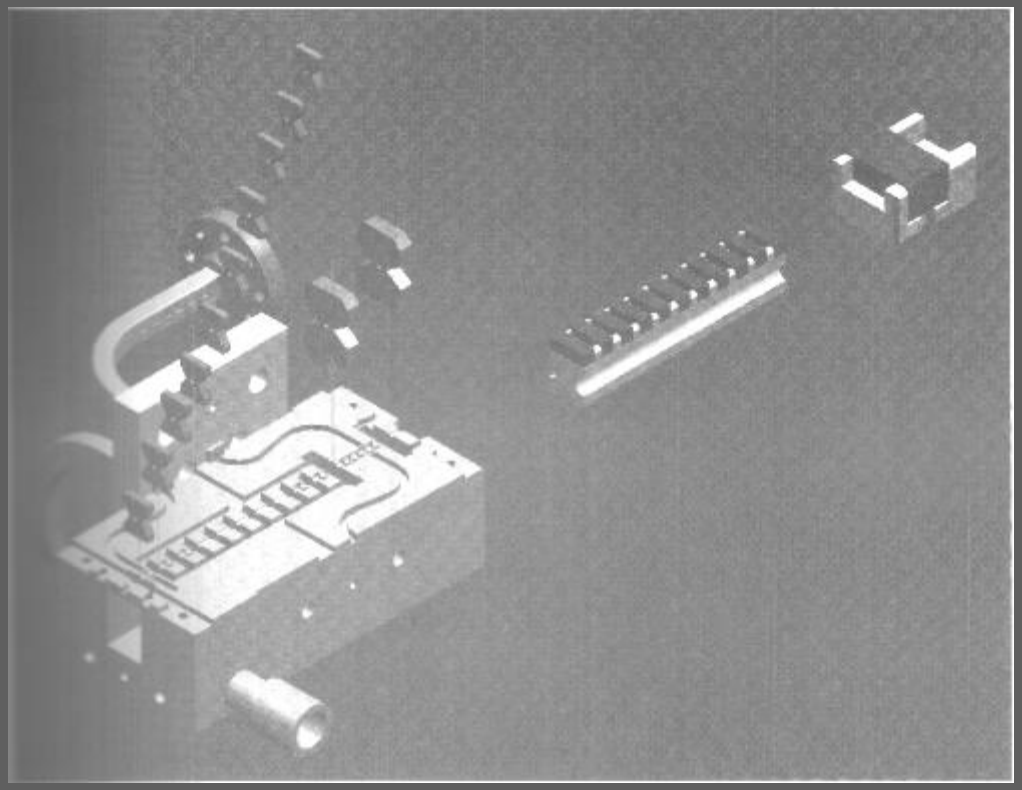

Explored model of klystrino circuit assembly with PPM pole pieces and magnet.

VIRCATOR (Group 3)

Virtual Cathode oscillator (vircator): Simple, no magnetic field required, single-shot device, low cost, tunable by controlling the space-charge density

Bremsstrahlung device in an electrostatic field realised in a waveguide resonator

Virtual cathode forms beyond the anode at a distance equal to the anode-cathode spacing

Beam current > Space-charge limiting current

Space-charge limiting current in a metal drift tube:

Radial space-charge electric field (potential gradient) gives a radial electron velocity at the expense of longitudinally directed electron velocity. At the space-charge limiting current, the electrostatic potential energy corresponding to the potential difference between the beam and the drift tube equals the electron kinetic energy, and the beam electrons cannot propagate forward

Analogous to an *LC* oscillator generating microwaves, the virtual cathode acting as a capacitor *C* in storing the beam kinetic energy, and the beam current itself being like a time-varying current through an inductor *L*

Space-charge limiting current:

Hollow annular beam of radius r_b in a waveguide resonator of radius r_0

In the free-space region outside the hollow beam $(r_b \le r \le r_0)$

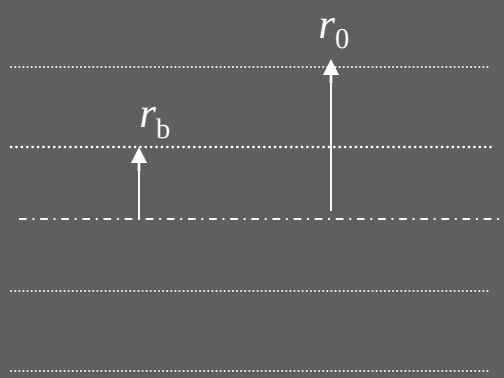

$$\varepsilon_0 E 2\pi r l = \rho_l l \qquad E = \frac{\rho_l}{2\pi\varepsilon_0 r}$$

$$E = -\frac{dV}{dr}$$

$$dV = -E dr = -\frac{\rho_l}{2\pi\varepsilon_0 r} dr \qquad \int dV = -\int \frac{\rho_l}{2\pi\varepsilon_0 r} dr$$

$$V = -\frac{\rho_l}{2\pi\varepsilon_0} \ln r + \text{Constant}$$

$V = 0$ at $r = r_0$

$$\text{Constant} = \frac{\rho_l}{2\pi\varepsilon_0} \ln r_0$$

$$V(r) = \frac{\rho_l}{2\pi\varepsilon_0} \ln \frac{r_0}{r}$$

$$\rho_l l = \rho l \alpha$$

$$\rho_l = \rho\alpha$$

$$J = \rho v_b$$

$$\frac{-I_b}{\alpha} = \rho v_b$$

$$\rho\alpha = \frac{-I_b}{v_b}$$

$$V(r) = \frac{\rho_l}{2\pi\varepsilon_0} \ln \frac{r_0}{r} = \frac{\rho\alpha}{2\pi\varepsilon_0} \ln \frac{r_0}{r} = \frac{-I_b}{2\pi\varepsilon_0 v_b} \ln \frac{r_0}{r} = \frac{I_b}{2\pi\varepsilon_0 v_b} \ln \frac{r}{r_0} \qquad (r_b \le r \le r_0)$$

In the free-space region inside the beam $0 \le r \le r_b$

$$E = 0$$

$$-\frac{dV}{dr} = 0 \qquad V = \text{constant} \qquad V(r_b) = \frac{I_b}{2\pi\varepsilon_0 v_b} \ln\frac{r_b}{r_0} = \text{constant}$$

$$V(r) = \frac{I_b}{2\pi\varepsilon_0 v_b} \ln\left(\frac{r}{r_0}\right) \quad (r_b \le r \le r_0)$$

$$= \frac{I_b}{2\pi\varepsilon_0 v_b} \ln\left(\frac{r_b}{r_0}\right) \quad (0 \le r \le r_b)$$

The cathode is at a negative potential $-V_c$ with respect to the anode-cum-waveguide resonator

For electron beam transport to make just possible, the relativistic kinetic energy of the beam should be just greater than the potential energy of the beam with respect to the zero potential of the waveguide wall. At the transition, the condition for the virtual cathode to form, may be written as

$$eV(r_b) = \gamma_c mc^2 - \gamma_b mc^2 = mc^2(\gamma_c - \gamma_b) \qquad \ge 0$$

$$eV(r_b) = \gamma_c mc^2 - \gamma_b mc^2 = mc^2(\gamma_c - \gamma_b) \qquad \geq 0$$

$$e\frac{I_b}{2\pi\varepsilon_0 v_b}\ln(\frac{r_b}{r_0}) = mc^2(\gamma_c - \gamma_b) \qquad \geq 0$$

$$e\frac{I_b}{2\pi\varepsilon_0 v_b}\frac{\gamma_b}{\sqrt{\gamma_b{}^2 - 1}}\ln(\frac{r_b}{r_0}) = mc^2(\gamma_c - \gamma_b) \qquad \geq 0$$

$$I_b = \frac{2\times 2\pi\varepsilon_0(\gamma_b{}^2 - 1)^{1/2} mc^3(\gamma_c - \gamma_b)}{\gamma_b e 2\ln(\frac{r_b}{r_0})} \qquad \geq 0$$

$$= \frac{2\times 2\pi\varepsilon_0(\gamma_b{}^2 - 1)^{1/2} mc^3(\gamma_c - \gamma_b)}{\gamma_b |e| 2\ln(\frac{r_0}{r_b})} \qquad \geq 0$$

$$I_b = \frac{4\pi\varepsilon_0 mc^3}{|e|2\ln(\frac{r_0}{r_b})}(\gamma_b{}^2 - 1)^{1/2}(\frac{\gamma_c - \gamma_b}{\gamma_b}) \qquad \geq 0$$

$$I_b = \frac{I_A}{2\ln(\frac{r_0}{r_b})}(\gamma_b{}^2 - 1)^{1/2}(\frac{\gamma_c - \gamma_b}{\gamma_b}) \qquad \geq 0$$

$$I_A = \frac{4\pi\varepsilon_0 mc^3}{|e|} = 17.1kA$$

$$\gamma_c mc^2 - mc^2 = |e|V_c$$

$$mc^2(\gamma_c - 1) = |e|V_c$$

$$\gamma_c = 1 + \frac{|e|V_c}{mc^2}$$

$$\gamma_b = \frac{1}{\sqrt{1 - \frac{v_b{}^2}{c^2}}}$$

$$v_b = \frac{\sqrt{\gamma_b{}^2 - 1}}{\gamma_b}c$$

$$I_b = \frac{4\pi\varepsilon_0 mc^3}{|e|2\ln(\frac{r_0}{r_b})}(\gamma_b{}^2 - 1)^{1/2}(\frac{\gamma_c - \gamma_b}{\gamma_b}) \qquad \geq 0$$

$$I_b = \frac{I_A}{2\ln(\frac{r_0}{r_b})}(\gamma_b{}^2 - 1)^{1/2}(\frac{\gamma_c - \gamma_b}{\gamma_b}) \qquad \geq 0$$

I_b attains maximum for $\gamma_b = \gamma_c{}^{1/3}$

$$I_{SC} = I_b\big|_{\max} = \frac{I_A}{2\ln(\frac{r_0}{r_b})}(\gamma_c{}^{2/3} - 1)^{3/2} \qquad I_A = \frac{4\pi\varepsilon_0 mc^3}{|e|} = 17.1kA$$

$$I_{SC} = \frac{I_A}{2\ln(\frac{r_0}{r_b})}(\gamma_c{}^{2/3} - 1)^{3/2} = \frac{8.5}{\ln(\frac{r_0}{r_b})}(\gamma_c{}^{2/3} - 1)^{3/2}\ kA \qquad \text{(hollow annular beam)}$$

$$I_{SC} = \frac{8.5}{\ln(\frac{r_0}{r_b})}(\gamma_c{}^{2/3} - 1)^{3/2}\ kA \quad \text{(hollow annular beam)}$$

$$I_{SC} = \frac{8.5}{1+\ln(\frac{r_0}{r_b})}(\gamma_c{}^{2/3} - 1)^{3/2}\ kA \quad \text{(solid annular beam)}$$

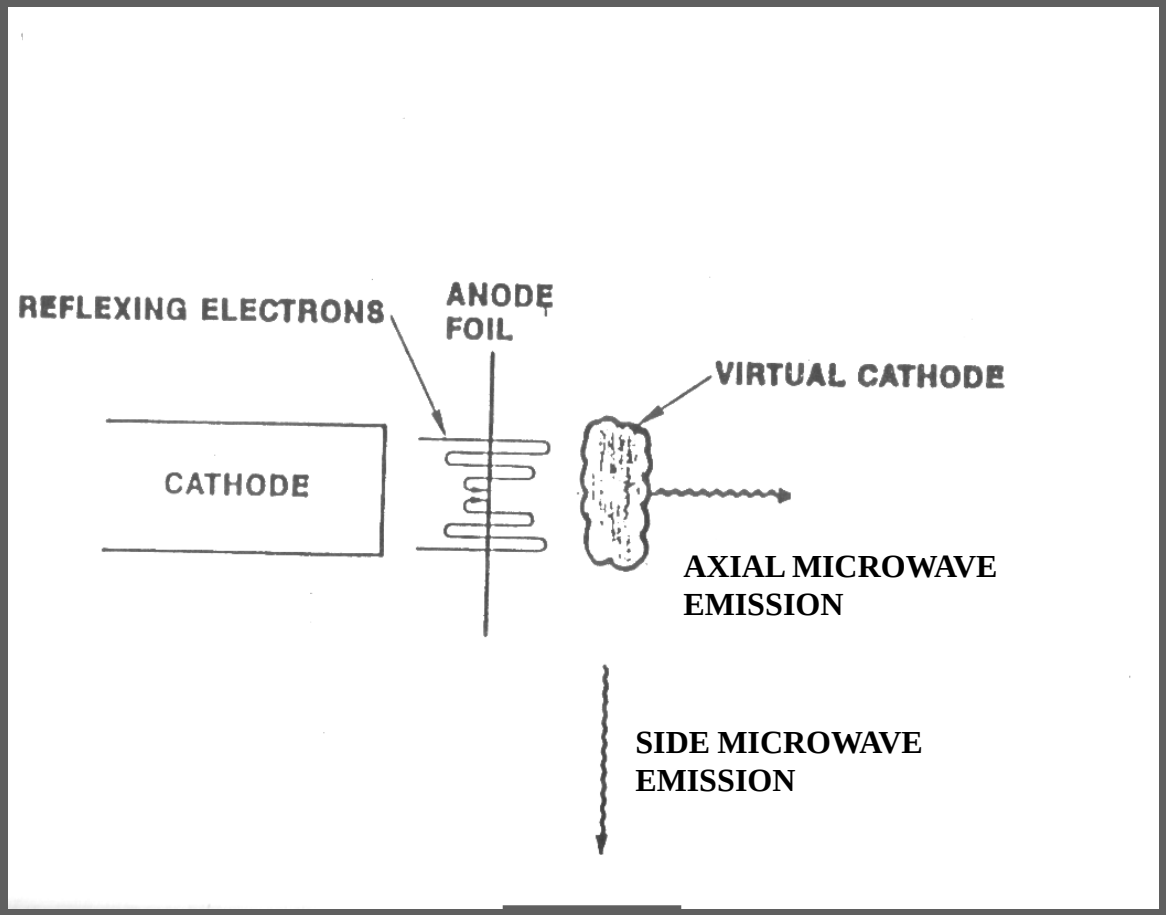

Oscillation occurs in both the location and the potential of the virtual cathode producing microwave radiation (virtual cathode oscillation) at f_{vc} estimated between f_p and 2.5 f_p.

$$f_p = \frac{\omega_p}{2\pi} = \frac{\sqrt{\frac{|\eta||\rho_0|}{\varepsilon_0}}}{2\pi}$$

$$|J| = |\rho_0| v_z = |\rho_0| \beta c$$

$$f_p\,(\mathrm{GHz}) \cong 4.08 \sqrt{\frac{|J|\,(\mathrm{kA/cm^2})}{\beta\gamma}}$$

Microwave emissions from either virtual cathode oscillation or from reflex oscillation or both take place. The efficiency of the device increases if

$$(f_{\mathrm{reflex}} \approx f_{vc})$$

$$f_{reflex} = \frac{1}{4\int_0^{d_{AK}} \frac{dz}{v_z}}$$

VIRCATOR (Group 3) (continued)

Types:

Axial extraction (TM mode)

Transverse extraction (TE mode)

Coaxial structure

Reditron (with the anode foil replaced by a thick metal anode with large holes)

Typical output parameters:

1 GW, 400-800 MHz, 75-125 ns, 100 J, single shot (220 lb)
400 MW, 435-544 MHz, ≤140 ns, 56 J, single shot (500 lb)
1GW, 2-4 GHz, 30 ns, 50 J, single shot (220 lb)

Typical beam voltage and current: 200 kV-6.5 kV; 10-100 kA (25 ns-1.7 μs)

Other typical reported specifications:

20 GW below 1 GHz; 7.5 GW at 1.7 GHz; 4 GW in C-band; 1 GW in X-band; 0.5 GW at 17 GHz

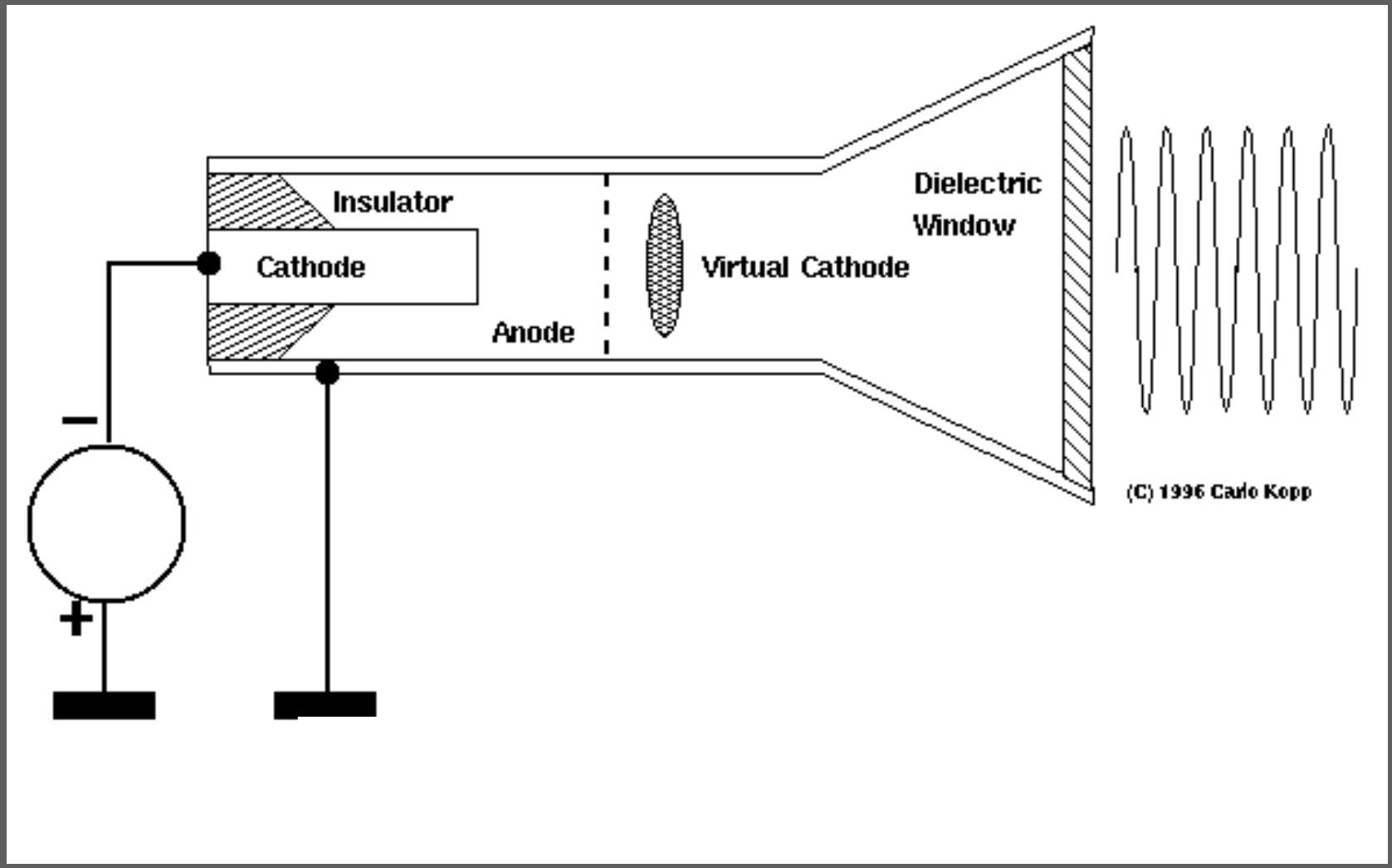

Virtual cathode oscillator or VIRCATOR

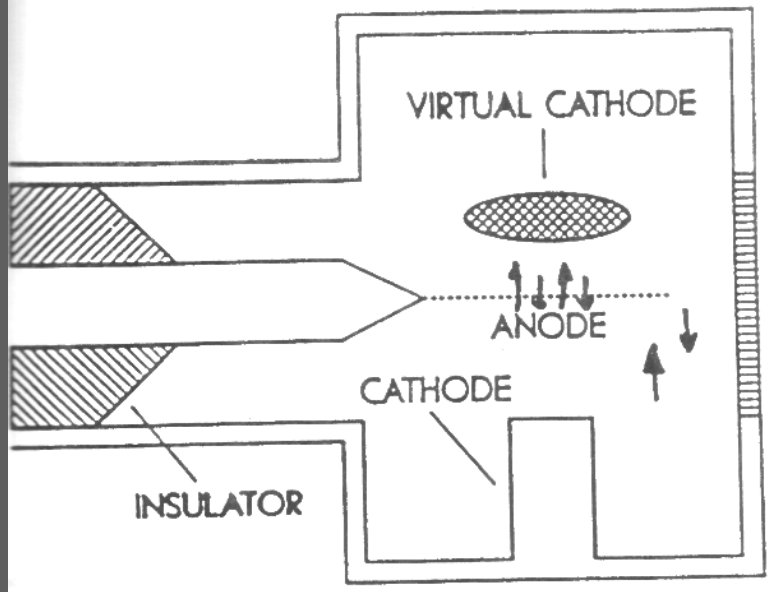

SIDE
EXTRACTION

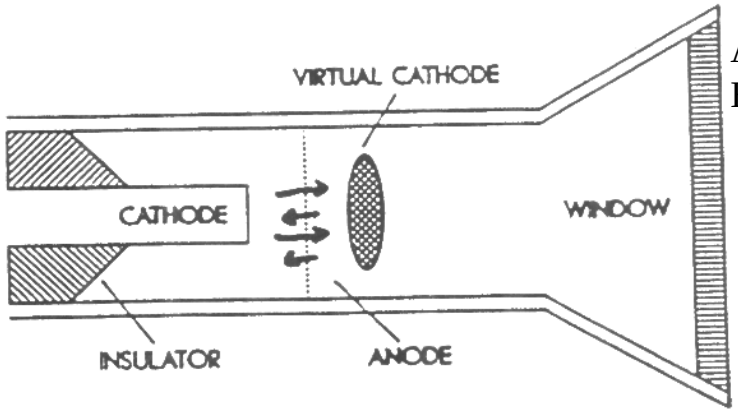

AXIAL
EXTRACTION

Anode is made of aluminum or titanium foil through which the electron beam, emitted typically by explosive field emission graphite cathode, is injected into the microwave interaction region of the vircator

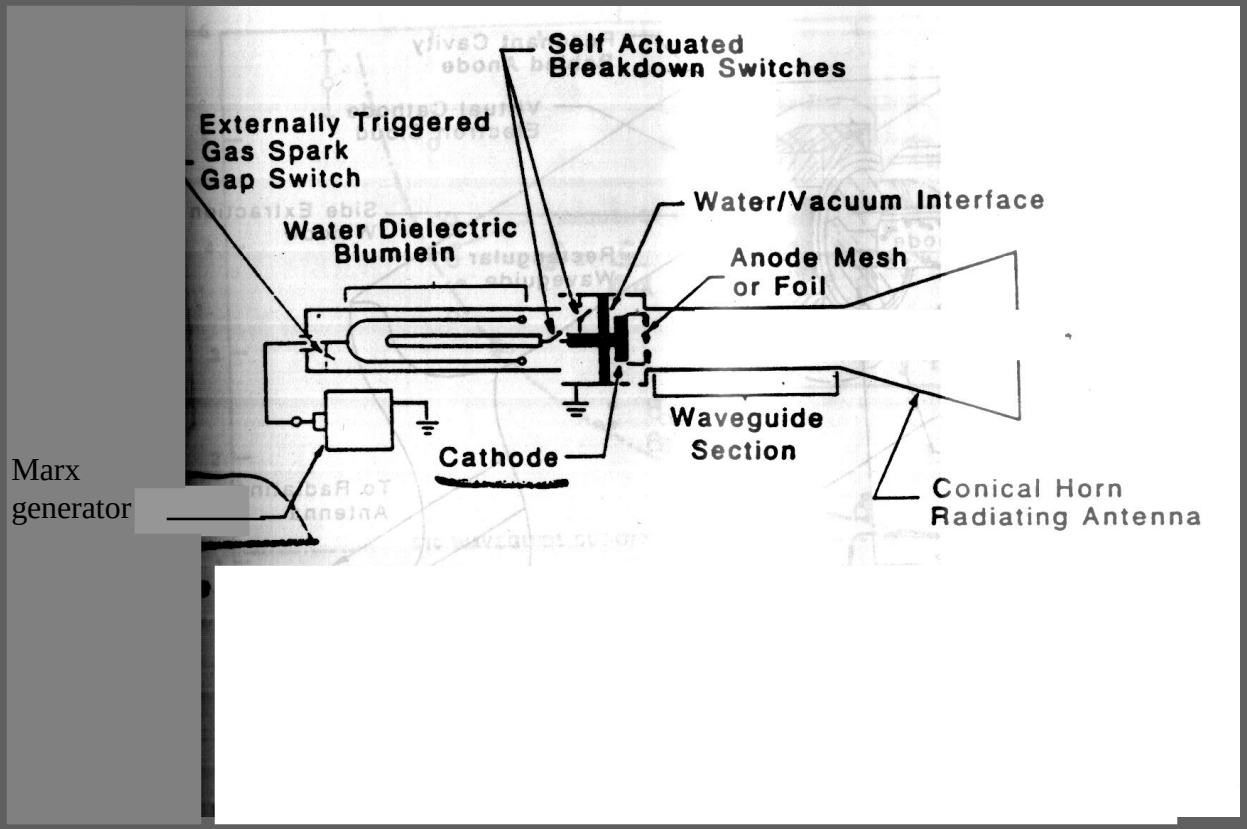

Marx generator feeding an IREB diode of a vircator

HPM cathodes

Explosive field emission cathode

Non-explosive field emission cathode

Thermionic emission cathode

Photoemission cathode

Explosive field emission cathode:

Emission kA/cm^2 due to ~ 100 kV/cm electric field from naturally occurring micro-points (materials: graphite, aluminum, stainless steel)

Pressure ~10^{-4}

Field emission current heats micro-points which rapidly heat and explode to form plasma flares within a few ns

Individual flares expand and merge within a 5-20 ms to form uniform emitter

(Electrons are drawn from the plasma)

Reusable from shot to shot

Difficulty: Gap closure shorting out the accelerating voltage

Non-explosive field emission cathode:

Pressure ~10^{-4}

Emission 100 A/cm^2-kA/ cm^2 from arrays of tungsten needle, grooved graphite, cesium iodide coated carbon fibre, common velvet, cloth, ferroelectric (such as PLZT ceramic of dielectric constant ~ 500) etc. (PLZT– Pb, La, Zr, Ti)

(Large local external electric field > $5x10^9$ GV/m pulls in free charges from the surroundings to the surface of the ferroelectric. The space charge, shielding the PLZT surface from the external electric field , is controlled by applying a rapidly changing electric field, to cause emission from the surplus charge thus forming pulsed electron beams)

Operates at fields below those required for explosive emission

No gap closure

Thermionic emission cathode:

Pressure: 10^{-9} Torr

Tungsten (mp: 3370 C; work function: 4.6 eV, 0.5 A/cm^2 at 2200 C)

Tantalum (mp: 2850 C; work function: 4.1 eV, 10 A/cm^2 at 2200 C)

Thoriated tungsten (work function: 2.6 eV, 3 A/cm^2 at 2200 C used in microwave oven magnetron)

Oxide-coated cathode:

100's of mA/cm^2 CW and 10's of A/cm^2 pulsed at 650-700 C

A mixture of barium, strontium, and calcium carbonates coated on nickel cylinder doped with zinc, tungsten, zirconium, or magnesium activator. Carbonates reduced to oxides by activation by passing large heater current and drawing current to the anode. Barium oxide and free barium (work function 1.6 eV) (obtained by reduction) reduces the overall work function to provide emission at lower temperature

Scandate cathode:

100 A/cm^2 at 1995 C

Cermet cathodes coated with a layer of $Sc_2 O_3$

B-type dispenser cathode:

~A's/cm^2 at 1100 C

:Porous tungsten impregnated with a mixture of BaO, CaO, and Al_2O_3

$$W + 3\ Ba_3Al_2O_6 + 6\ CaO = 3\ Ba_2CaAl_2O_6 + Ca_3WO_6 + 3\ Ba$$

M-type dispenser cathode: B-type coated with a thin layer of osmium-iridium or osmium-ruthenium to reduce the operating temperature by ~ 90 C

MM-type dispenser : Mixed metal matrix in which the enhancing material is put in the tungsten matrix

Photoemission cathode:

Emission 100-200 A/cm^2 from laser illuminated Ga As, Cs_3 Sb, LaB_6

Tuned off and on by laser pulse

Pressure: 10^{-10} Torr

Relativistic TWT (Group 3)

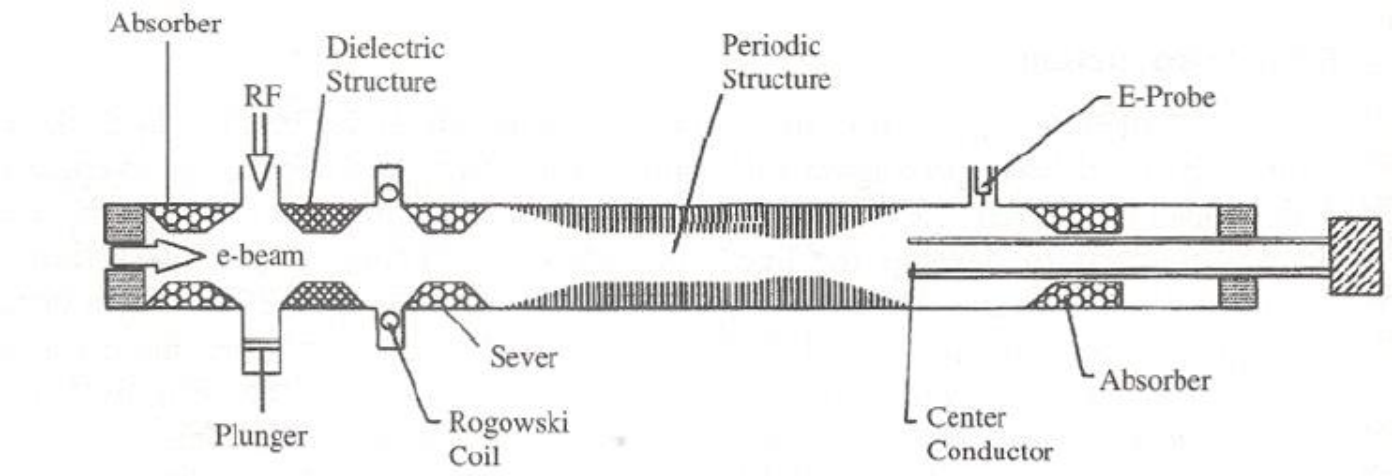

Figure 5.1 Typical TWT experimental arrangement showing the two amplifier stages separated by a sever.

Capable of delivering large RF power due to high beam voltage/ high beam power

Larger dimensions due to high beam voltage

Synchronisation is maintained even if significant reduction in beam kinetic energy takes place

MILO (Group 3)

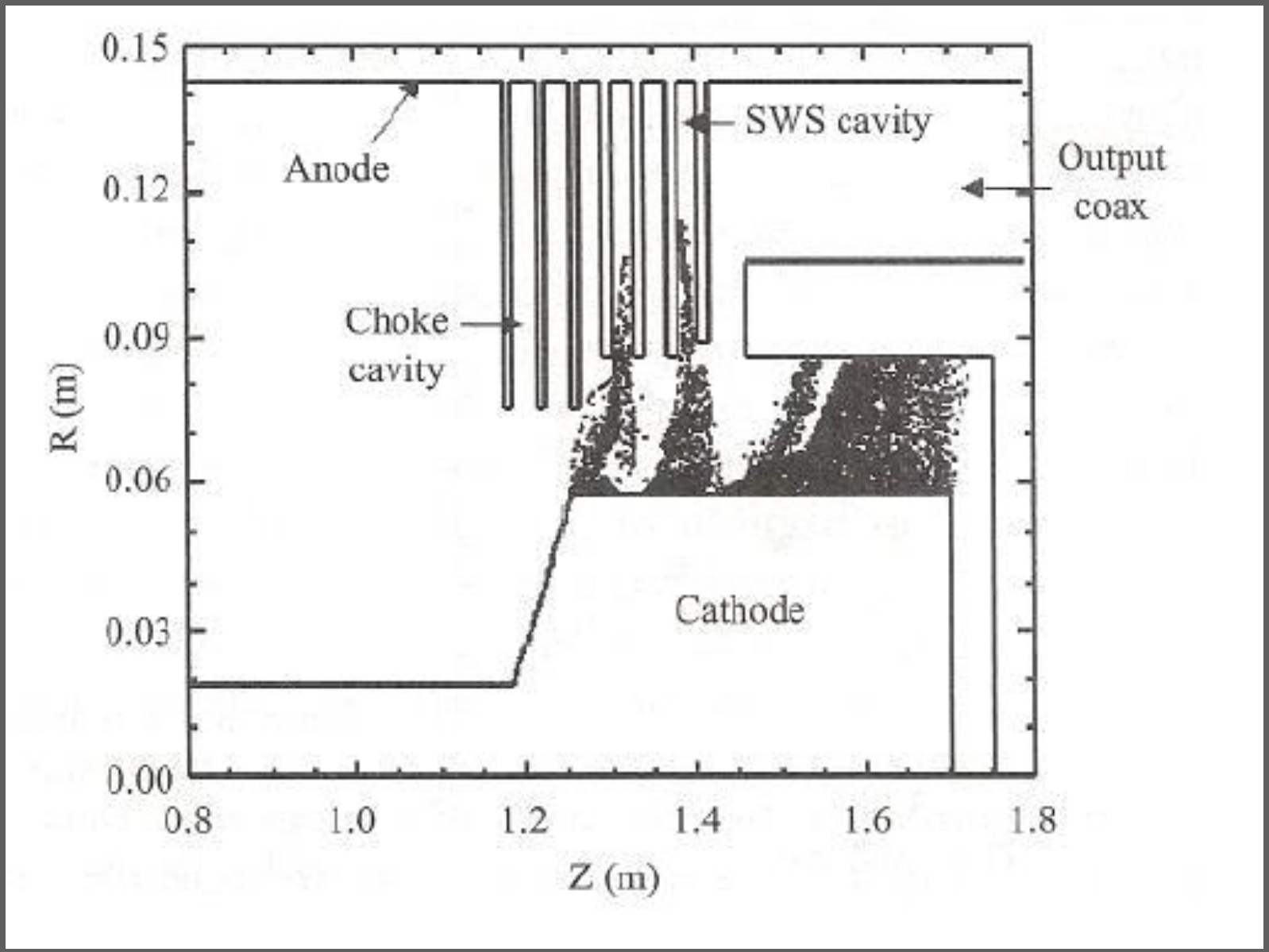
0.15
0.12
0.09
0.06
0.03
0.00
R (m)
0.8
1.0
1.2
1.4
1.6
1.8
Z (m)
Anode
SWS cavity
Output coax
Choke cavity
Cathode

MILO (Group 3)

Magnetically insulated line oscillator — MILO

A crossed-field device but requires no external magnetic field

- unlike a magnetron

Self-generated magnetic field

Intrinsic electron current generates azimuthal magnetic field

Azimuthal magnetic field inhibits electron flow from reaching the anode prior to oscillation (provides self insulation)

Self-insulating property inhibits electrical breakdown of the anode-to-cathode gap

- Can handle 10-100's of GW at a voltage of 100's of kV.

Typical MILO experimental parameters:

- 50 MW, 75 ns; 300 MW, 10 ns

Tapered MILO for better efficiency and output power

- First group (4-5) uniform cavities define the oscillation frequency
- Second group of tapered cavities increase the group velocity, amplifies microwave signal and transforms into a travelling-wave mode in the output line.
- Placement of the diode within the slow-wave region allows for energy recovery from the diode circuit.

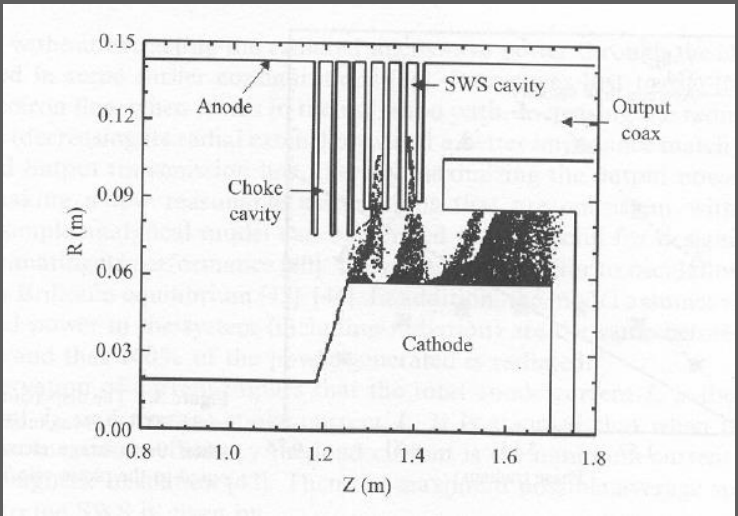
0.15
0.12
0.09
0.06
0.03
0.00
R (m)
0.8
1.0
1.2
1.4
1.6
1.8
Z (m)
Anode
SWS cavity
Output coax
Choke cavity
Cathode

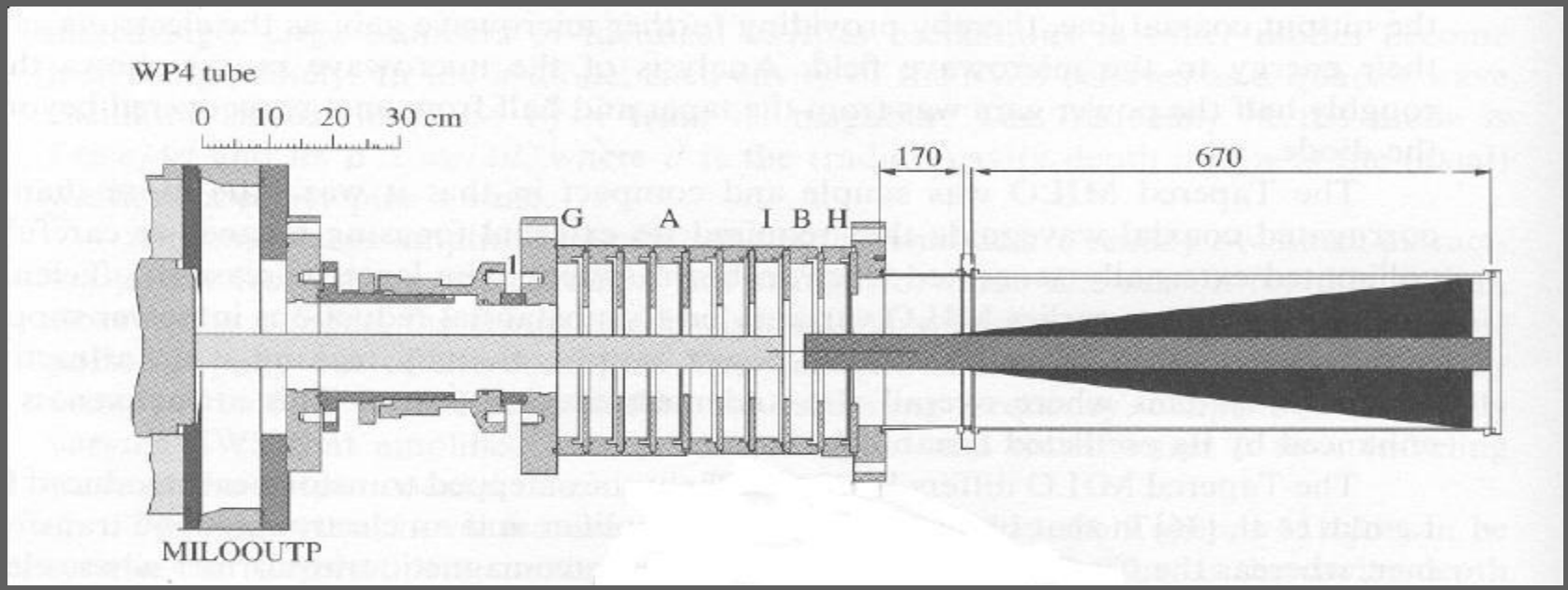
WP4 tube
0 10 20 30 cm
170
670
G
A
I
B
H
MILOOUTP

Orotron (RDG), MWCG, and MWDG (Group 3)

RDG — Radiation diffraction generator (Orotron)

SWO — Surface-wave oscillator

BWO — Backward-wave oscillator

MWCG — Multi-wave Cerenkov generator

MWDG — Multi-wave diffraction generator

All can be realised in a forward-fundamental slow-wave structure (rippled waveguide).

SWO and RDG each operate very close to wave group velocity $v_g \cong 0$.

BWO operates at a negative v_g .

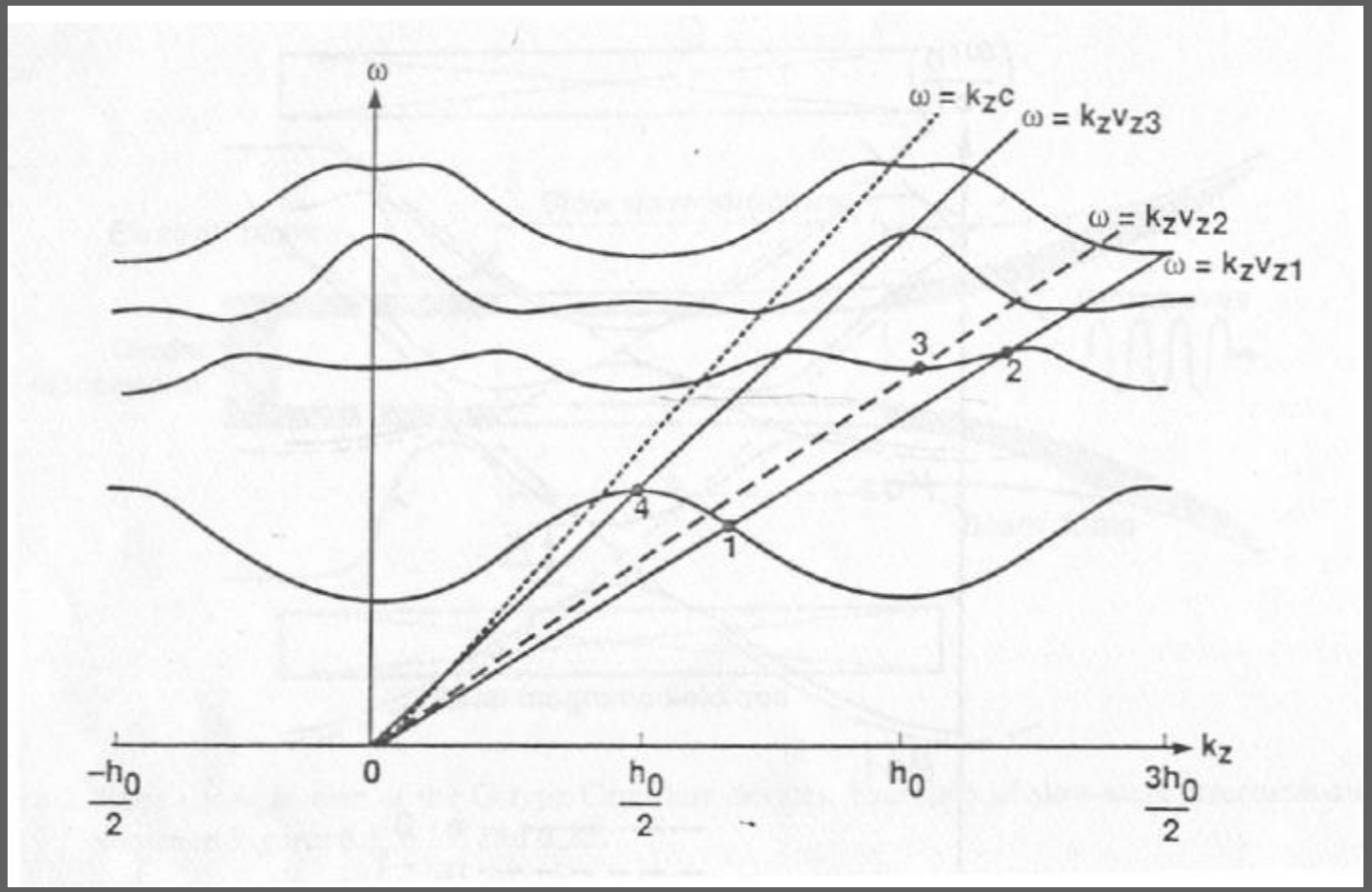
ω
ω = k_z c
ω = k_z v_z3
ω = k_z v_z2
ω = k_z v_z1
3
2
4
1
k_z
−h_0/2
0
h_0/2
h_0
3h_0/2

SWO (Group 3)

Operates at the upper-edge frequency of the passband of the lowest order mode.

$v_g \cong 0$

$k_z z_0 = \pi$ (phase shift between consecutive waveguide ripples)

k_z = axial phase propagation constant

z_0 = axial periodicity of waveguide ripples

$h_o = 2\pi / z_0$

RDG (Orotron) (Group 3)

Operates at the lower-edge frequency of the passband of a higher order mode, and at a higher frequency as well as at higher phase propagation constant than SWO.

$v_g \cong 0$

$k_z z_0 = 2\pi$ (phase shift between consecutive waveguide ripples)

Orotron (RDG) (Group 3)

Open resonator formed by a pair of mirrors
Sheet beam close to the grating-surface plane mirror
Radiation perpendicular to the axis ($v_g \cong 0$)
Output through a hole on the curved-surface mirror

Reported output:
100 MW at 8.6 mm wavelength with 10% efficiency
50 MW at 5.5 mm wavelength with 5% efficiency

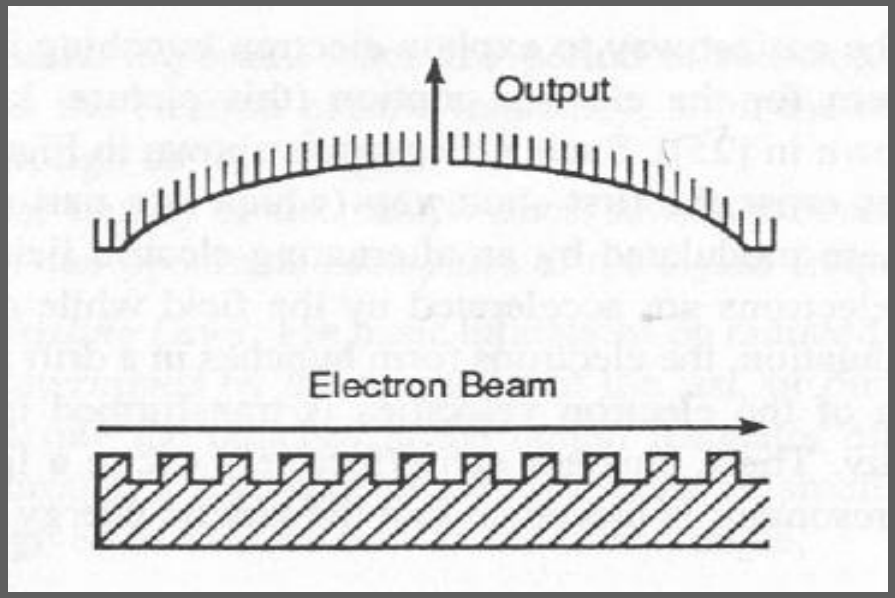

MWCG (Group 3)

High power, over-sized, over-moded device ($D/\lambda >> 1$)
Three-section tube
Sectioning or severing of slow-wave structures aids in mode selection
First section: rippled (corrugated) section operating as an SWO
Second section: drift section above cutoff (unlike in a klystron)
Third section: rippled (corrugated) section operating as an SWO

Same corrugation geometry and periodicity in the first and the third sections
Beam current less than the start-oscillation current for individual sections
Two sections in concert produce signal of narrow spectral width

Typical MWCG output power: 15 GW, 50% efficiency in X-band, 3 GW, 20% efficiency in Ka band

MWDG

Similar to MWCG except in the following respects:
First section: rippled (corrugated) section operating as a BWO
Second section: drift section above cutoff (unlike in a klystron)
Third section: rippled (corrugated) section operating as an RDG
Different corrugation geometries and periodicities in the first and the third sections

PASOTRON (Group 3)

Plasma-filled BWO
Plasma aids electron beam transport through the interaction region.
Plasma contributes to the improvement of coupling of the beam to the structure yielding higher efficiency.

Capable of repetitively fired operation and exceptionally reproducible shot-to-shot characteristics

Plasma-cathode electron gun to create a plasma-fill through impact ionization of the background gas, typically, 5 Torr helium

No magnetic field required: beam confined by its own magnetic field
Compact, lightweight

Slow-wave structure: Typically, 3.25 cm average radius, 0.715 cm ripple-depth, and 2.4 cm periodicity
A reflective iris positioned upstream for forward-wave RF extraction

Output: A typical L-band 200 kV PASOTRON produced 20 MW peak power (1 kJ per pulse)

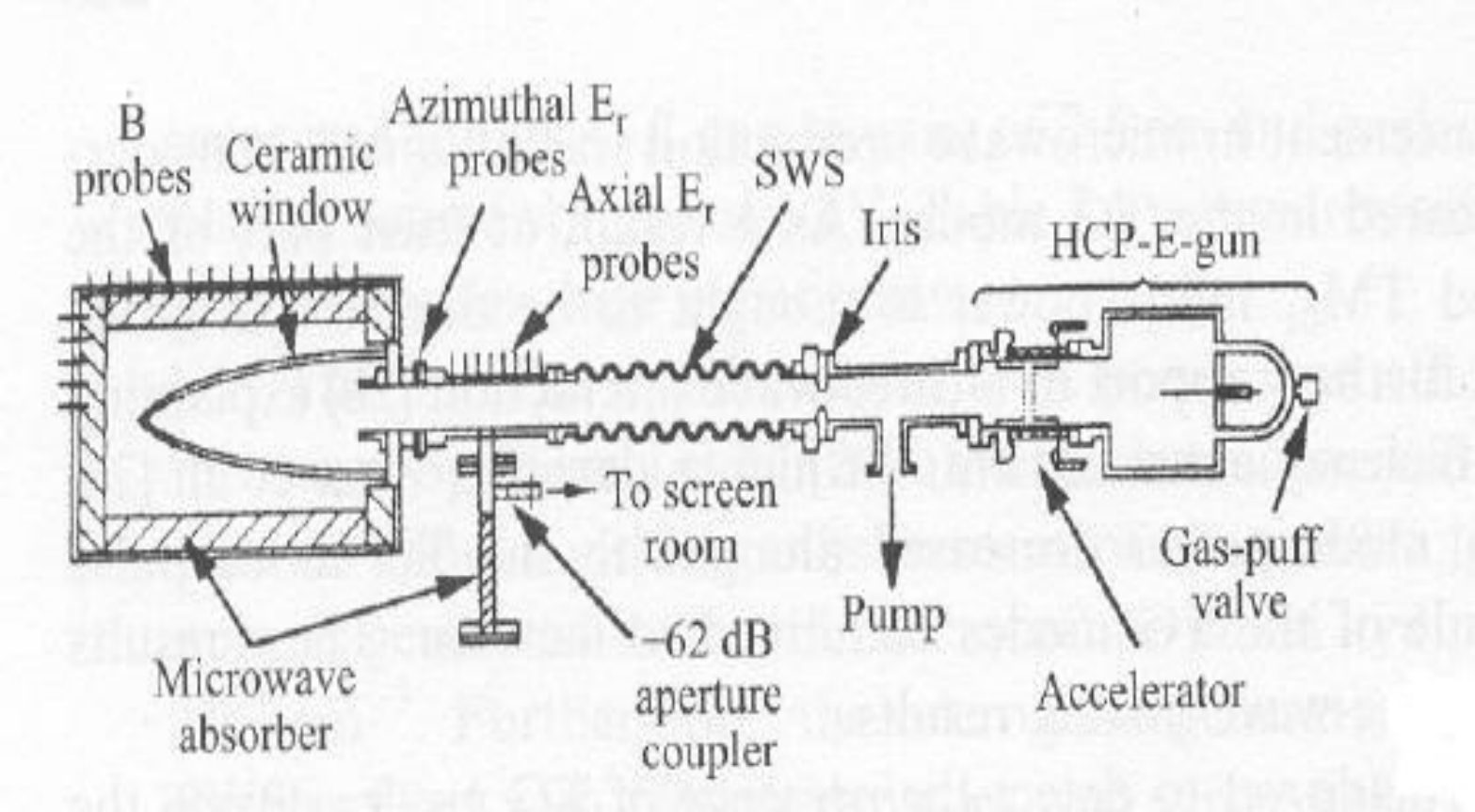
B
probes
Ceramic
window
Azimuthal E_r
probes
Axial E_r
probes
SWS
Iris
HCP-E-gun
To screen
room
Pump
Gas-puff
valve
Microwave
absorber
−62 dB
aperture
coupler
Accelerator

Pasotron

RELTRON (Group 3)

State-of-the-art variant of relativistic klystron — reliable, flexible, cost-effective, compact, high-power source

Advantage in terms of the powers per unit size and unit weight

Basic parts and features:

- Voltage injector to produce high current beam; Multi-cavity (typically, two-cavity) beam buncher; Post-acceleration gap (that reduces energy spread of electrons in the bunch; Output cavities (low-Q) for converting high beam power into microwave power.
- High electronic efficiency (40-50%)
- Frequency determined by the physical dimensions of the modulating cavities
- Large frequency tuning (>15%)
- Compact tube size because of short bunching distance
- Straightforward output coupling to deliver power directly through the fundamental TE_{10} mode in a standard rectangular waveguide
- No external magnetic field required for high peak power RELTRON
- Small permanent magnets required for high average power RELTRON

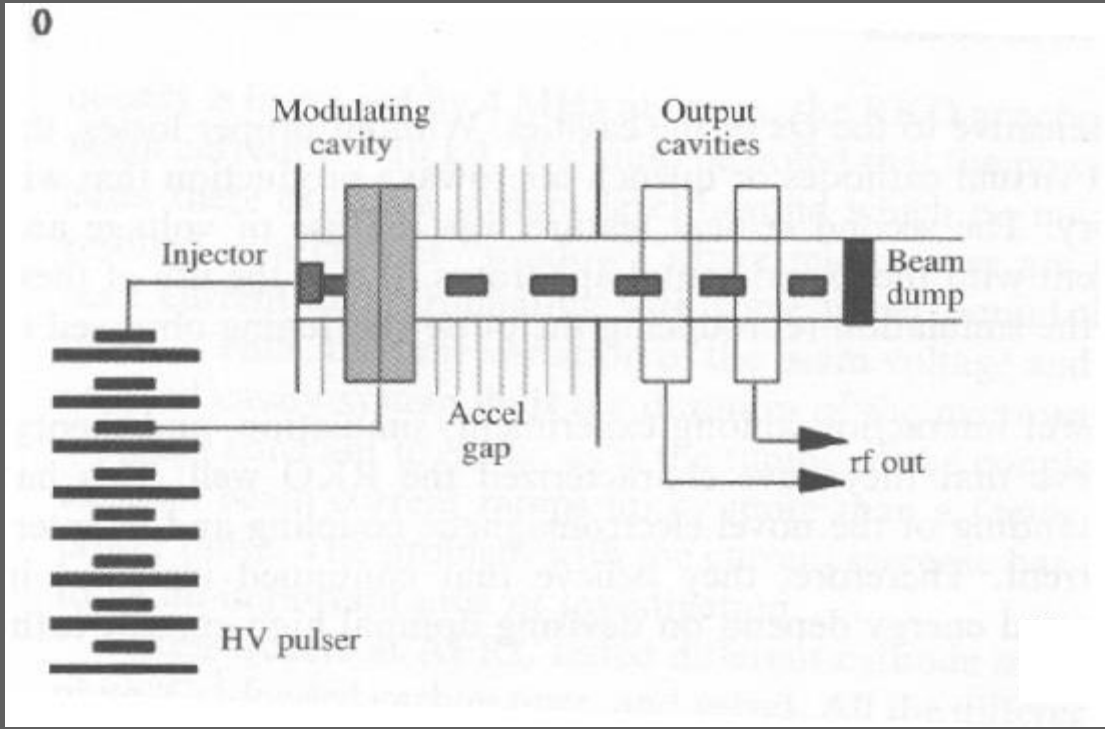
Modulating cavity
Output cavities
Injector
Beam dump
Accel gap
rf out
HV pulser

Reltron

Reltron parameters:

L-band: 400-500 MW (rms)
Beam injector voltage = 800 kV
Beam current = 1.1 kA
Post-acceleration voltage = 800 kV
Efficiency > 40%
100’s of J’s of energy per pulse (flat-top pulse duration of a few nanoseconds)
Peak power > 1 GW driven by 1.5 MV voltage pulse

Typical HPM Devices (Group 3)	Pulsed power (GW)	Energy per pulse (J)
RELTRON	0.5	300
MILO	1.5	330
RKA	10	1000
PASOTRON	0.005	500
MWCG	15	900
VIRCATOR	1	50

Fast-wave tubes

Size of interaction structures of conventional and gyro devices

Conventional TWT using a helix slow-wave structure

Axial phase propagation constant β

Radial propagation constant $\gamma = (\beta^2 - k^2)^{1/2} \approx \beta = \omega / v_p$

(under slow-wave assumption)

Gain versus (a quantity proportional to frequency) characteristics shows peak typically at

$$\gamma a = 1.6 \Rightarrow \beta a = 1.6$$

$$\Rightarrow \frac{\omega}{v_p} a = 1.6 \qquad \Rightarrow \frac{2\pi f}{v_p} a = 1.6 \qquad \Rightarrow \frac{2\pi f}{\frac{v_p}{c} c} a = 1.6$$

$$\Rightarrow \frac{2\pi f}{\frac{v_p}{c} c} a = 1.6 \quad \text{Putting} \quad \frac{v_p}{c} = \frac{1}{10} \quad \Rightarrow \frac{2\pi \times 10}{\frac{c}{f}} a = 1.6$$

$$\Rightarrow \frac{2\pi \times 10}{\lambda} a = 1.6 \qquad \Rightarrow \quad a = \frac{1.6\lambda}{2\pi \times 10} \sim 0.025 \ \lambda$$

Size of interaction structures (*Continued*)

Gyro-device using a fast-wave circular waveguide

Eigenvalue: TE_{01} mode

$$k_c\, a = 3.832$$

$$\frac{\omega_c}{c}\, a = 3.832$$

$$\Rightarrow \frac{2\pi\, f_c}{c}\, a = 3.832$$

$$\Rightarrow\ a = \frac{3.832\ c}{2\pi\, f_c} \approx \frac{3.832\ c}{2\pi\, f} = \frac{3.832\ c}{2\pi\, f} = \frac{3.832\ \lambda}{2\pi} \sim 0.61\lambda \quad (\text{Putting } f \cong f_c)$$

For 35 GHz:

$$\lambda \approx 8.57\, mm \qquad a \approx 5.2\, mm$$

Eigenvalue: TE_{02} mode

$$k_c a = 7.016$$

For 42 GHz: $\lambda \approx 7.14\,mm$

$$a = \frac{7.016\lambda}{2\pi} \sim 1.12\lambda \qquad a \approx 7.9\,mm$$

TE_{01} waveguide radius is (0.61λ/0.025 λ)~25 times helix radius

TE_{02} waveguide radius is (1.12λ/0.025 λ)~45 times helix radius

Increased sizes for over-moded waveguides

Non-relativistic axial bunching in a helix TWT

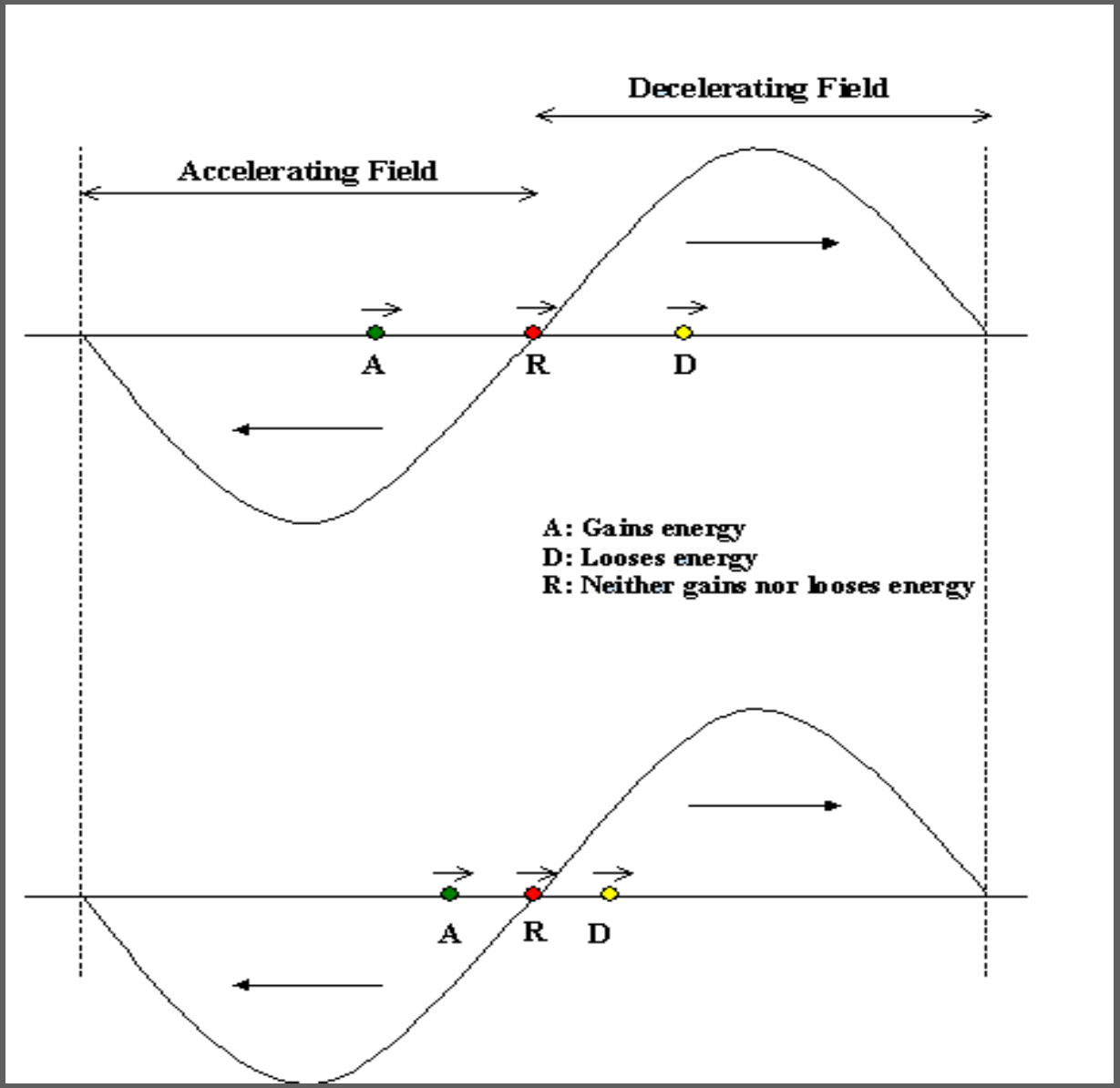

Near-synchronism for net energy transfer from the beam to RF waves:

$$v_0 \gtrsim v_{ph}$$

Relativistic azimuthal bunching in a gyro-device

$$\omega_c = \frac{|e|B}{\gamma m}$$

γ increases

ω_c decreases

T_c increases

Electron in accelerating RF electric field moves slower in circular orbit

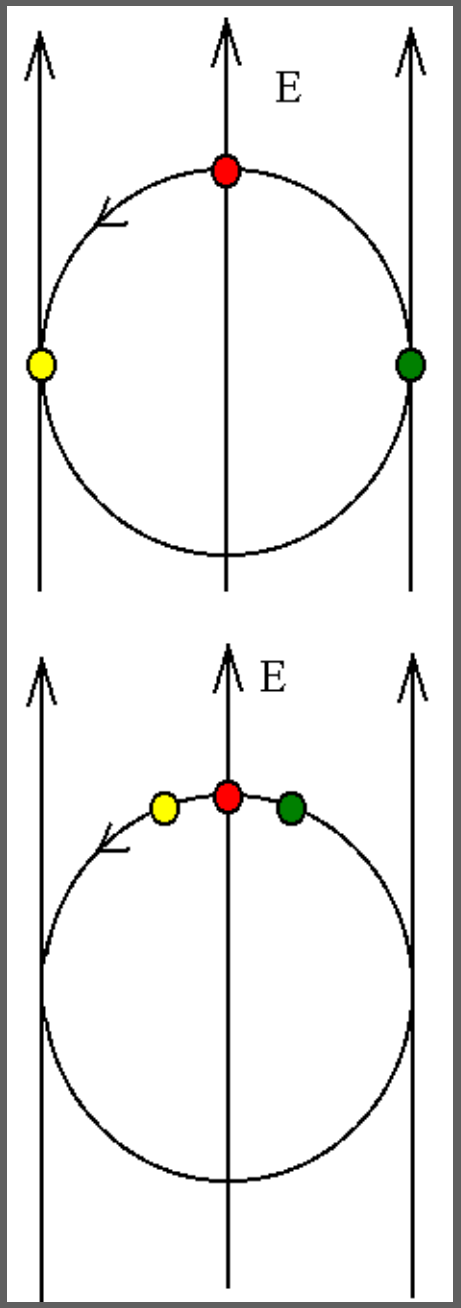

$$\omega_c = \frac{|e|B}{\gamma m}$$

γ decreases

ω_c increases

T_c decreases

Electron in decelerating RF electric field moves faster in circular orbit

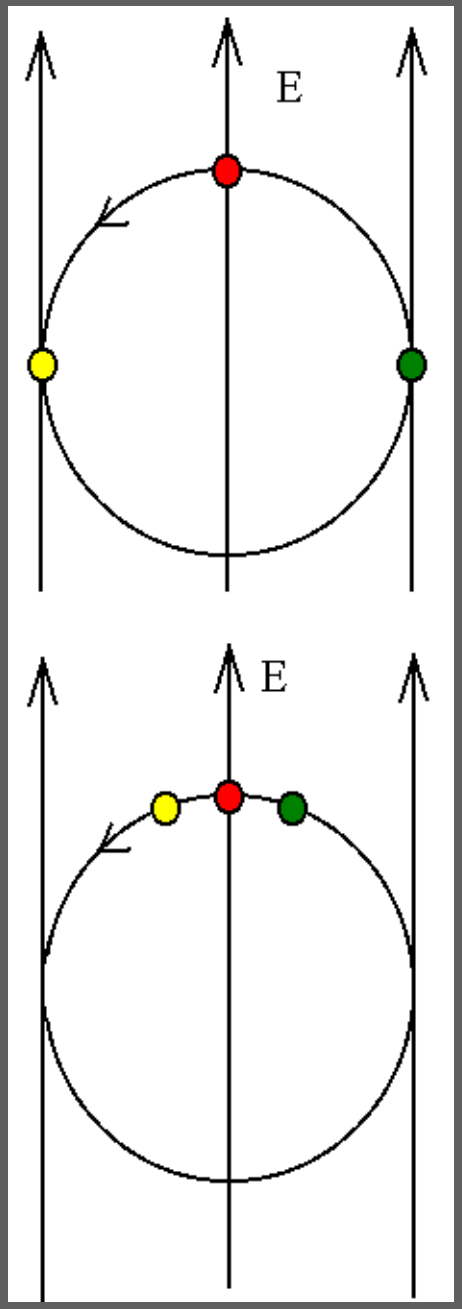

Near-cyclotron resonance for net energy transfer from the beam to RF waves:

$T_c \gtrsim T$

or

$\omega_c \lesssim \omega$

Space-charge waves

$$J = \rho v \qquad J = J_0 + J_1 \qquad \rho = \rho_0 + \rho_1 \qquad v = v_0 + v_1$$

$$J_0 = \rho_0 v_0$$

$$J_1 = \rho_0 v_1 + v_0 \rho_1 \qquad \frac{\partial J_1}{\partial z} = \rho_0 \frac{\partial v_1}{\partial z} + v_0 \frac{\partial \rho_1}{\partial z} \qquad \frac{\partial J_1}{\partial z} + \frac{\partial \rho_1}{\partial t} = 0$$

$$-\frac{\partial \rho_1}{\partial t} = \rho_0 \frac{\partial v_1}{\partial z} + v_0 \frac{\partial \rho_1}{\partial z} \qquad \frac{\partial \rho_1}{\partial t} + v_0 \frac{\partial \rho_1}{\partial z} = -\rho_0 \frac{\partial v_1}{\partial z}$$

$$D\rho_1 = -\rho_0 \frac{\partial v_1}{\partial z} \qquad D = \frac{\partial}{\partial t} + v_0 \frac{\partial}{\partial z}$$

$$\frac{dv_1}{dt} = \frac{e}{m} E_s = \eta E_s \qquad \frac{dv_1}{dt} = \frac{\partial v_1}{\partial t} + \frac{dz}{dt}\frac{\partial v_1}{\partial z} = \frac{\partial v_1}{\partial t} + v\frac{\partial v_1}{\partial z} = \frac{\partial v_1}{\partial t} + (v_0 + v_1)\frac{\partial v_1}{\partial z} = \frac{\partial v_1}{\partial t} + v_0 \frac{\partial v_1}{\partial z}$$

$$\frac{\partial v_1}{\partial t} + v_0 \frac{\partial v_1}{\partial z} = \eta E_s \qquad Dv_1 = \eta E_s \qquad \left[\frac{d}{dt} = \frac{\partial}{\partial t} + v_0 \frac{\partial}{\partial z} = D\right]$$

$$D\rho_1 = -\rho_0 \frac{\partial v_1}{\partial z}$$

$$Dv_1 = \eta E_s$$

$$D^2\rho_1 = -\rho_0 D\frac{\partial v_1}{\partial z} = -\rho_0 \frac{\partial}{\partial z} Dv_1 = -\rho_0 \frac{\partial}{\partial z}\eta E_s = -\eta\rho_0 \frac{\partial E_s}{\partial z}$$

$$\left[\frac{d}{dt} = \frac{\partial}{\partial t} + v_0 \frac{\partial}{\partial z} = D\right]$$

$$D^2\rho_1 = -\eta\rho_0 \frac{\partial E_s}{\partial z}$$

$$\frac{\partial E_s}{\partial z} = \frac{\rho_1}{\varepsilon_0}$$

RF quantities vary as $e^{j(\omega t - \beta z)}$

$$D = \frac{\partial}{\partial t} + v_0 \frac{\partial}{\partial z} = j\omega - j\beta v_0 = j(\omega - \beta v_0)$$

$$D^2\rho_1 = -\eta\rho_0 \frac{\rho_1}{\varepsilon_0} = \frac{-\eta\rho_0}{\varepsilon_0}\rho_1 = \frac{-|\eta||\rho_0|}{\varepsilon_0}\rho_1 = -\omega_p{}^2\rho_1$$

$$D^2 = -\omega_p{}^2$$

$$\left[\frac{|\eta||\rho_0|}{\varepsilon_0} = \omega_p{}^2\right]$$

$$D = \pm j\omega_p$$

$$\omega - \beta v_0 = \pm\omega_p$$

$$\omega - \beta v_0 \mp \omega_p = 0$$

Dispersion relation for space-charge waves

Cyclotron waves

$$m\frac{dv_{1x}}{dt} = e(\vec{v}\times\vec{B})_x$$

$$m\frac{dv_{1y}}{dt} = e(\vec{v}\times\vec{B})_y$$

$$\vec{v}\times\vec{B} = \begin{vmatrix} \vec{a}_x & \vec{a}_y & \vec{a}_z \\ v_x & v_y & v_z \\ B_x & B_y & B_z \end{vmatrix}$$

$$B_x = 0,\ B_y = 0,\ B_z = B$$

$$\frac{dv_{1x}}{dt} = \frac{e}{m}(\vec{v}\times\vec{B})_x = \eta(\vec{v}\times\vec{B})_x$$

$$[\frac{d}{dt} = \frac{\partial}{\partial t} + v_0\frac{\partial}{\partial z} = D]$$

$$Dv_{1x} == \eta(\vec{v}\times\vec{B})_x$$

$$Dv_{1y} == \eta(\vec{v}\times\vec{B})_y$$

$$Dv_{1x} = \eta B v_y = -\omega_c v_y \qquad [\omega_c = -\eta B] \qquad Dv_{1y} = -\eta B v_x = \omega_c v_{1x}$$

$$D^2 v_{1x} = -\omega_c D v_{1y} = -\omega_c(\omega_c v_{1x}) = -\omega_c{}^2 v_{1x}$$

$$D^2 = -\omega_c{}^2 \qquad \omega - \beta v_0 \mp \omega_c = 0$$

Dispersion relation for cyclotron waves

Space-charge and cyclotron waves

Space-charge waves

$$\beta = \beta_e \mp \beta_p$$

Cyclotron waves

$$\beta = \beta_e \mp \beta_c$$

Upper sign for the fast wave, and lower sign for the slow wave

$$\beta_e = \frac{\omega}{v_0}$$

$$\beta_e = \frac{\omega}{v_0}$$

$$\beta_p = \frac{\omega_p}{v_0}$$

$$\beta_c = \frac{\omega_c}{v_0}$$

$$\omega_p = \left(\frac{|\eta|\rho_0}{\varepsilon_0}\right)^{1/2}$$

$$\omega_c = |\eta| B$$

Space-charge and cyclotron waves (*continued*)

Space-charge waves

$$\beta = \beta_e \mp \beta_p$$

$$\beta = \frac{\omega}{v_p} = \frac{\omega}{v_0} \mp \frac{\omega_p}{v_0} = \frac{\omega \mp \omega_p}{v_0}$$

$$v_p = \frac{\omega}{\omega \mp \omega_p} v_0$$

$$\omega - \beta v_0 \mp \omega_p = 0$$

Cyclotron waves

$$\beta = \beta_e \mp \beta_c$$

$$\beta = \frac{\omega}{v_p} = \frac{\omega}{v_0} \mp \frac{\omega_c}{v_0} = \frac{\omega \mp \omega_c}{v_0}$$

$$v_p = \frac{\omega}{\omega \mp \omega_c} v_0$$

$$\omega - \beta v_0 \mp \omega_c = 0$$

Upper sign for the fast wave, and lower sign for the slow wave

Amplification of space-charge waves

- An electron beam of uniform diameter in a resistive-wall cylindrical waveguide
- An electron beam in a rippled-wall (varying diameter) conducting-wall cylindrical waveguide
- An electron beam of varying diameter in a conducting-wall cylindrical waveguide
- An electron beam mixed with another beam of a slightly different DC electron beam velocity (two-stream amplifier)
- An electron beam penetrating through a plasma (beam-plasma amplifier)
- An electron beam interacting with RF waves supported by a slow-wave structure (TWT)

Intersection between slow space-charge and circuit waves

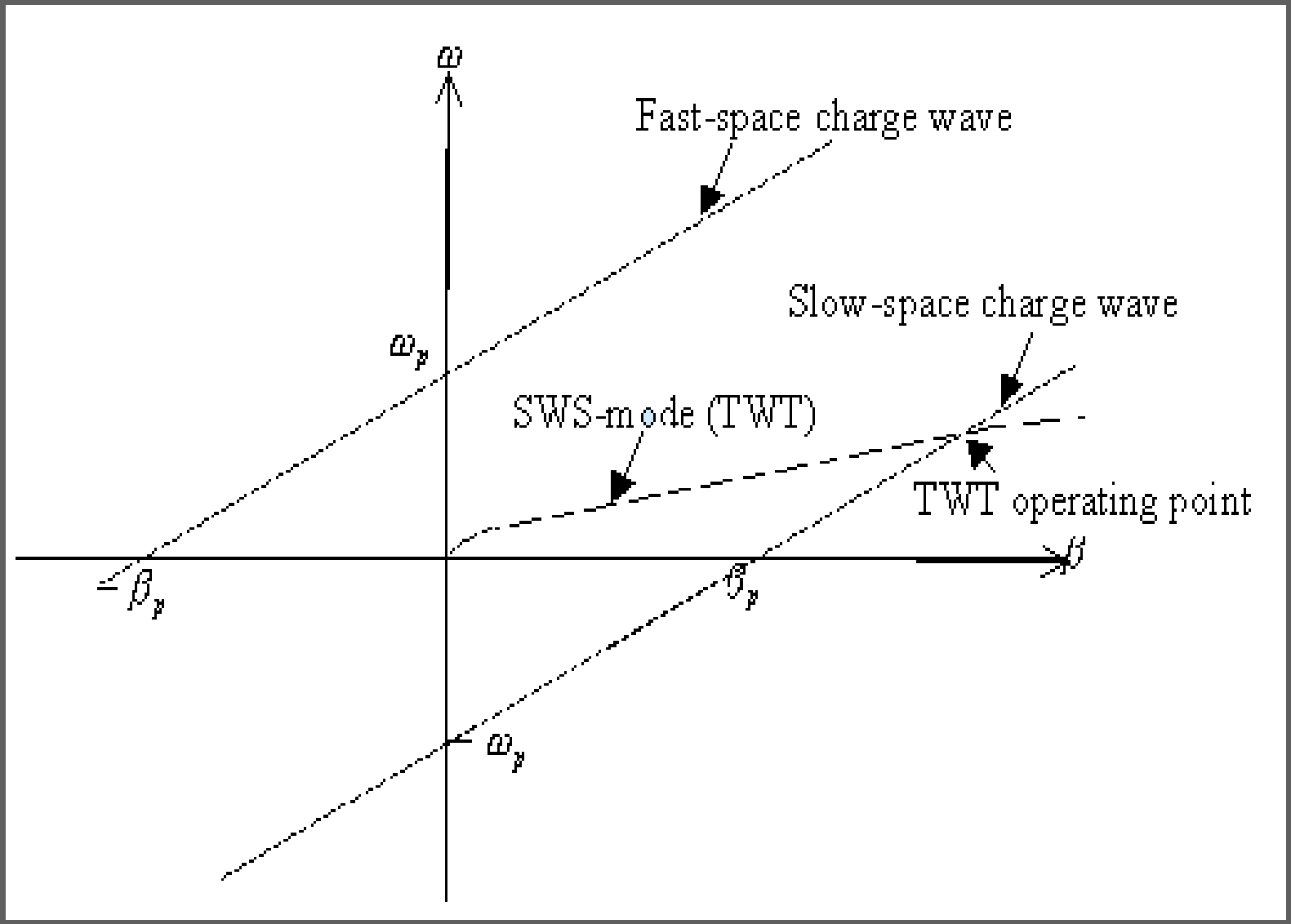

Intersection between fast-cyclotron and circuit waves

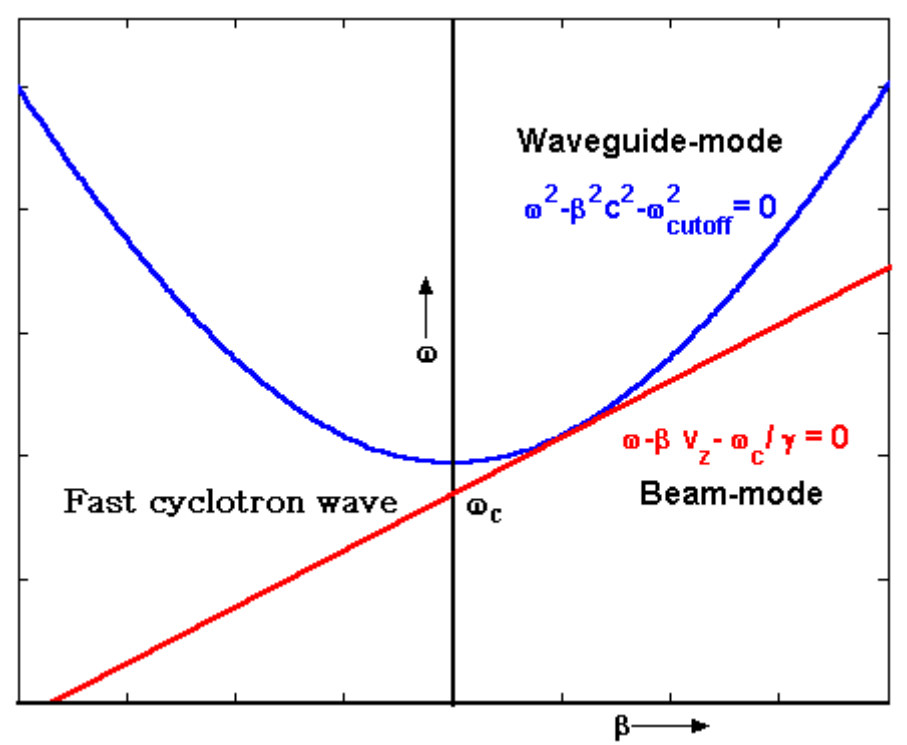

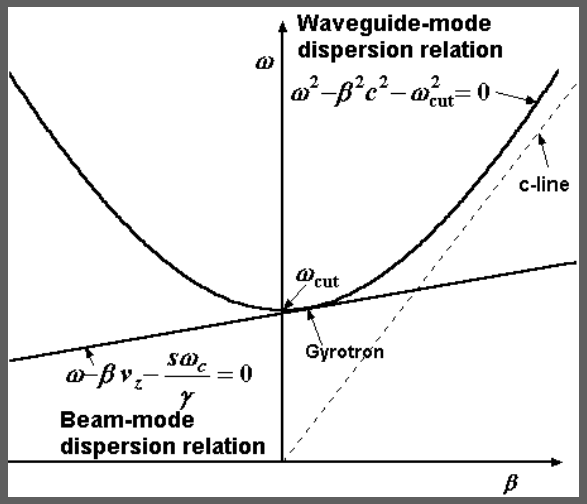

Gyrotron

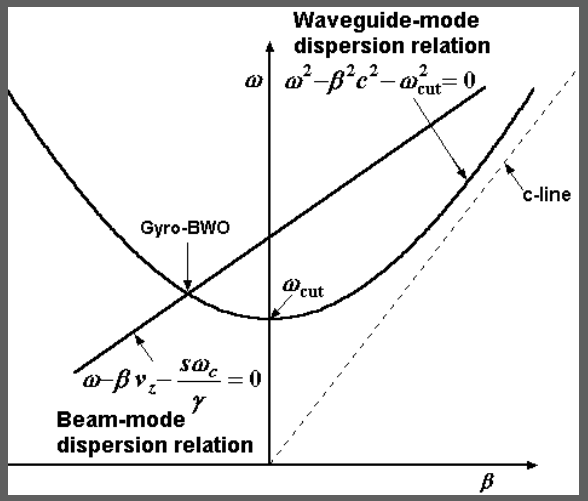

Gyro-BWO

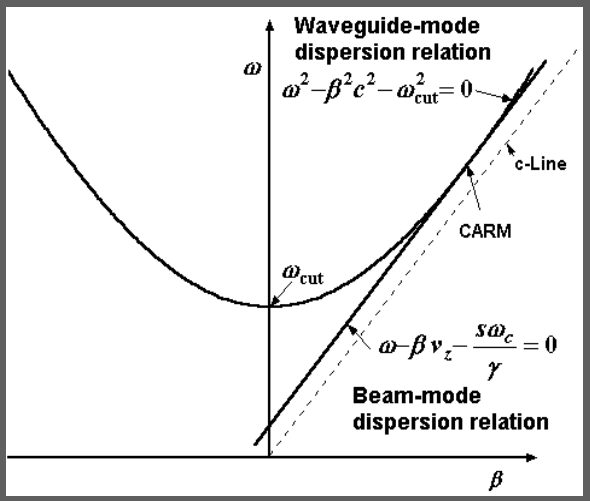

CARM

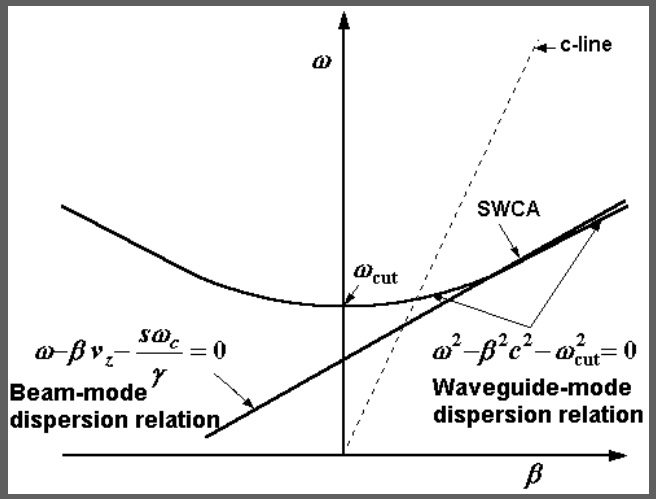

SWCA

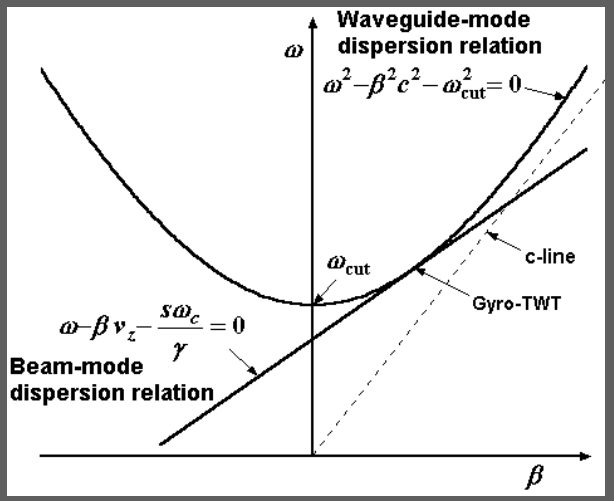

Gyro-TWT

Plots of beam-mode and waveguide-mode dispersion characteristics showing the operating point as the intersection between these plots (*Prepared by Vishal Kesari <vishal_kesari@rediffmail.com>*)

Gyrotron (Group 4)

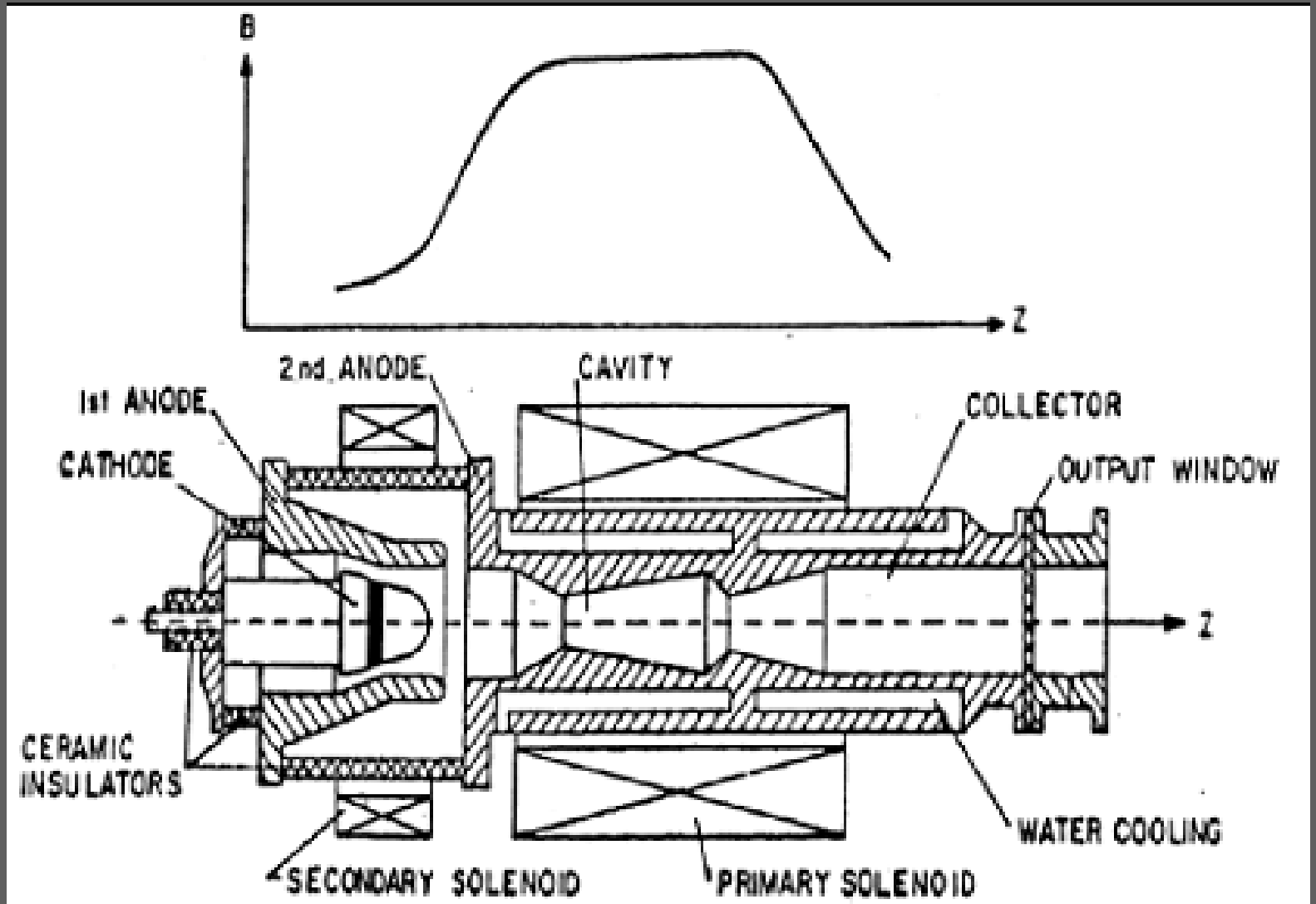

Ref: Kisel' et. al., Radio Eng. Electron. Phys., 19, No.4, 95 (1974)

Gyrotron (Group 4) (*continued*)

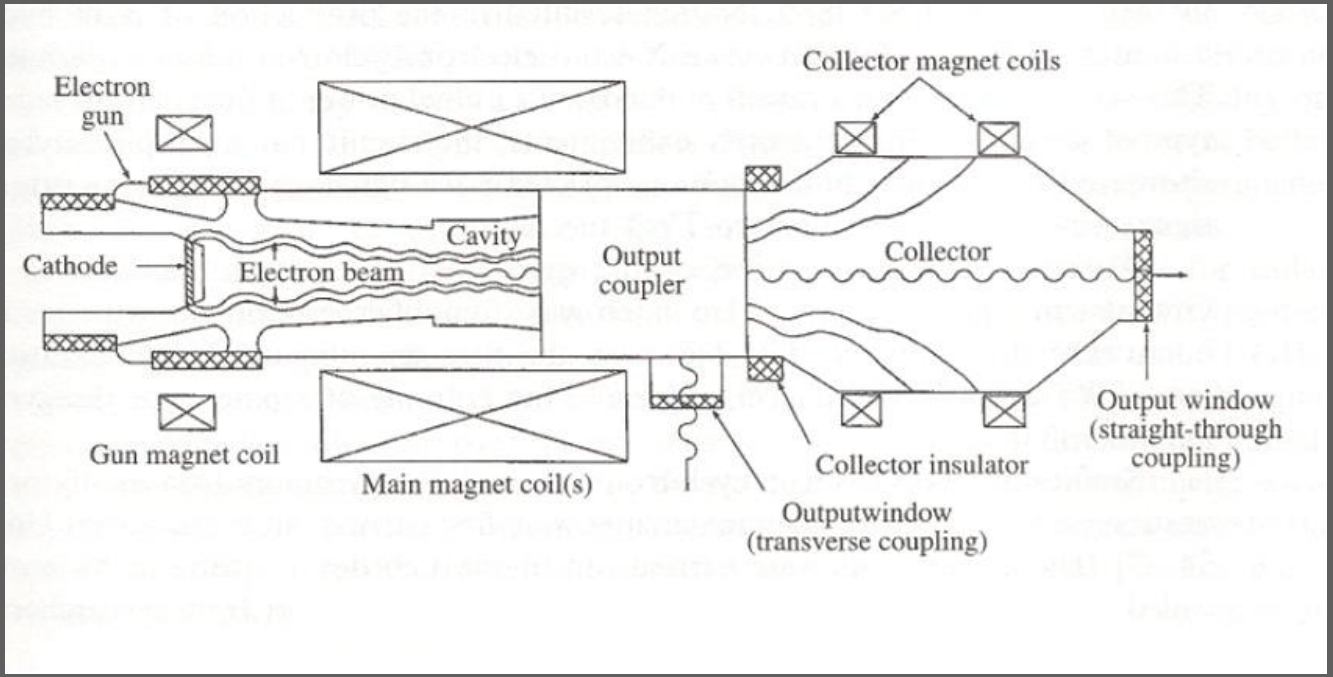

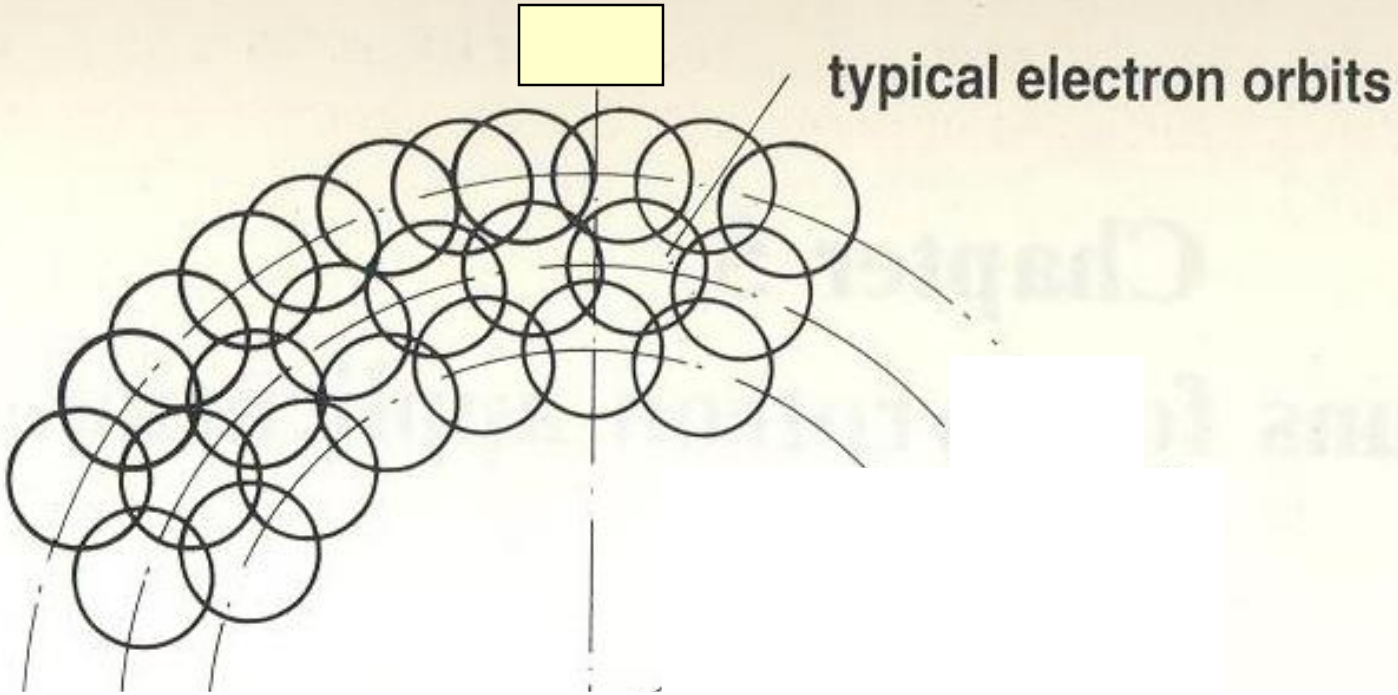
typical electron orbits

Gyrotron (Group 4) (*continued*)

Fixed-frequency oscillator

Weakly relativistic hollow electron beam with beamlets in helical trajectory with high transverse energies

Beam interacts with TE mode of a waveguide, usually cylindrical

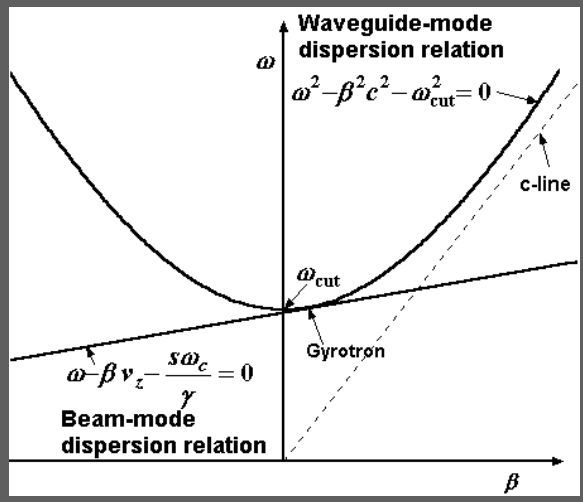

Gyro-TWT operating point

$$\omega_c = eB_0 / m$$

$\omega - \beta v_0 - \omega_c = 0$ (for fast cyclotron wave)

Interpreting ω_c as the relativistic cyclotron angular frequency ω_c/γ

Beam-mode dispersion relation:

$$\omega - \beta v_z - \omega_c / \gamma = 0$$

For small Doppler shift βv_z :

$$\omega \cong \omega_c / \gamma$$

Gyrotron (Group 4) (*continued*)

For small Doppler shift: $\omega \cong \omega_c / \gamma$

$\omega_c = eB_0 / m \quad \Rightarrow \quad B_0 = 3.57 \times 10^{-11} \gamma$ Tesla/ hertz of cyclotron frequency

$\gamma mc^2 - mc^2 = |e| V_0 \quad \Rightarrow \quad \gamma = 1 + \dfrac{|e| V_0}{mc^2}$ (Relativistic mass factor)

Waveguide-mode dispersion relation: $\omega^2 - \beta^2 c^2 - \omega_{\text{cut}}{}^2 = 0$

$\beta L = \pi \quad \Rightarrow \quad \beta = \dfrac{\pi}{L} \quad \Rightarrow \quad \omega^2 = \dfrac{\pi^2}{L^2} c^2 + \omega_{\text{cut}}{}^2$

Taking, typically, $L = 6\lambda_{\text{cut}} = \dfrac{6c}{f_{\text{cut}}} = \dfrac{6c}{\omega_{\text{cut}}} 2\pi \quad \Rightarrow \quad \omega^2 = \dfrac{\omega_{\text{cut}}^2}{4 \times 36} + \omega_{\text{cut}}^2$

$\Rightarrow \quad \omega = 1.03 \omega_{\text{cut}}$

Operating mode chosen close to the cutoff

$v_{ph} (= \omega / \beta) >> c \qquad v_g (= \dfrac{\partial \omega}{\partial \beta}) \approx 0$

Gyrotron (Group 4) (*continued*)

$v_g \left(= \frac{\partial \omega}{\partial \beta}\right)$ close to zero makes

Energy velocity slow enough to keep enough electromagnetic energy in the cavity to provide the field for beam-wave interaction

Propagation constant β small, mitigating the effects of velocity spread in the electron beam on the inhomogeneous broadening of the cyclotron resonance band

Even a small down tapering of the waveguide radius on the cathode side effective in making the cutoff frequency in this region larger than the operating frequency thereby preventing electromagnetic radiation from entering the cathode region

Interaction structure

Smooth waveguides instead of periodic structures

Beam not located close to structure boundary

Less reduction of waveguide size with frequency as compared to a slow-wave structure

Larger interaction volume, allowing higher power operation, with reduced wall loss density <2 kW/cm^2 particularly for CW and long-pulse operation

Over-sized waveguides for reduced wall loss density due to reduced field and increased wall area, though inviting mode competition

Number of resonant modes in a give frequency range proportional to the cavity radius

Cavity of diameter 5λ and length 6λ can support 30 modes in 1% frequency interval

Diffractive quality factor Q_d

$$Q_d = \omega \tau_d = \omega \frac{L}{v_g} = \omega \frac{L}{c^2 / v_p} = \frac{\omega L}{c^2} \frac{\omega}{\beta} = \frac{4\pi L^2}{\lambda^2}$$

[putting $\beta L = \pi, \quad v_p = \omega / \beta, \quad v_p v_g = c^2, \quad c = f\lambda$]

Q_d = diffractive quality factor

Q = quality factor

$$Q_d = \omega \tau_d \quad \Rightarrow \quad \omega = \frac{Q_d}{\tau_d} \quad \Rightarrow$$

$$Q = \omega \frac{W}{P}$$

ρ = reflection coefficient

$$= \frac{Q_d}{\tau_d} \frac{W}{P} = \frac{Q_d}{\frac{P \tau_d}{W}} = \frac{Q_d}{1 - \rho}$$

$$\left[\because \frac{P \tau_d}{W} = \frac{\text{Energy lost during the time energy travels out of cavity}}{\text{Energy stored in the cavity}} = \frac{1}{1 - \rho} \right]$$

$$Q = \frac{Q_d}{1 - \rho}$$

Waveguide modes

TE_{0p} mode:

Gives the smallest ohmic losses
Suffers from mode competition from the TE_{2p} mode

TE_{1p} mode

Suffers from greater wall losses
Space-charge depression of the beam potential due to the beam location near the waveguide axis
Modes degenerate in frequency for $p >> 1$

TE_{np} $(n >> p)$ whispering-gallery mode

Gives moderate wall losses
Reduced magnetic field as can be combined with high beam harmonic operation in large-orbit configuration
Reduced space-charge depression due to the placement of the beam near the cavity wall and reduced related beam velocity spread and efficiency enhancement

Magnetron injection gun (MIG)

Forms a hollow beam of electrons comprised of helical beamlets of small orbital radii compared to the transverse dimensions of the interaction structure of the device

Convex (conical) cathode operating in the temperature-limited region to minimise the velocity spread in the beam and prevent the formation of mirrored electrons at low values of the beam pitch factor and the consequent efficiency reduction

Electrons drawn off the cathode with a small angular velocity at an angle with the tube axis into a system of a crossed dc electric field, established by the first anode, and a magnetic field, established by the gun solenoid, and a large amount of axial velocity established by the second anode

Electrons subjected to a slowly increasing magnetic field, before entering the interaction region, ensuring small changes in electron motion during one gyro-cycle

Mode converter (optional) for changing from the interaction waveguide mode to the output waveguide mode

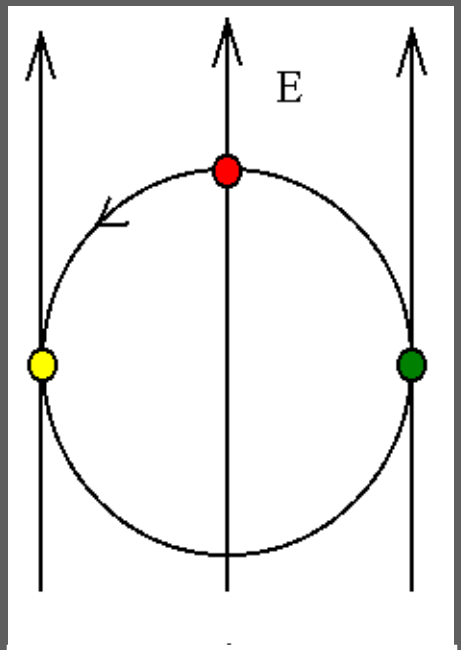

Fundamental operation

$\omega \cong \omega_c / \gamma$

$\omega \cong \omega_c$ (if ω_c represents the relativistic cyclotron angular frequency)

- An initially decelerated electron after half rotation will decelerate if the field reverses
- An initially accelerated electron after half rotation will accelerate if the field reverses

$T_c/2 = T/2$

$\Rightarrow \omega = \omega_c$

(fundamental operation)

Second harmonic operation

- **Initially (accelerated/)decelerated electron is (accelerated/) decelerated after half a rotation, if the field changes by a cycle**

$$\frac{T_c}{2} = T$$

$$T_c = 2T$$

$$\omega = 2\omega_c$$

Second cyclotron harmonic resonance (relativistic)

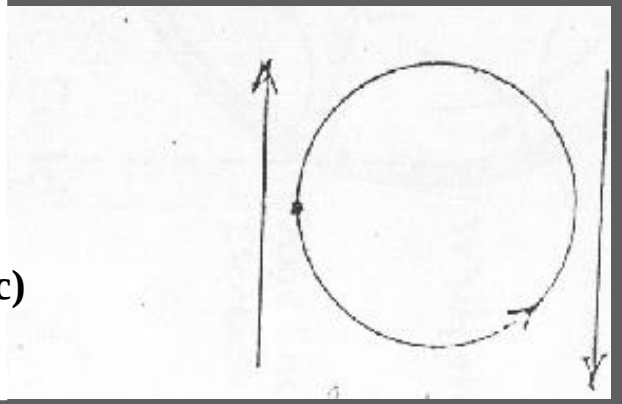

$$\omega - \beta v_z - \omega_c / \gamma = 0 \quad \Rightarrow \quad \omega \cong \omega_c / \gamma \quad \Rightarrow \quad \omega \cong \omega_c \quad \text{(relativistic)}$$

$$\omega - \beta v_z - 2\omega_c / \gamma = 0 \quad \Leftarrow \quad \omega \cong 2\omega_c / \gamma \quad \Leftarrow \quad \omega \cong 2\omega_c \quad \text{(relativistic)}$$

In general,

$\omega - \beta v_z - s\omega_c / \gamma = 0$, where s is the cyclotron harmonic or beam harmonic number

Unconventional Gyrotrons (Group 4)

Coaxial cavity gyrotrons
Vane-loaded gyrotrons in a magnetron-like structure
Quasi-optical gyrotron (QOG)
Large-orbit gyrotrons (LOG)

Some other gyro-devices (Group 4)

Gyro-TWT, Gyro-klystron, Gyro-twystron, Gyro-BWO, Harmonic multiplying gyro-TWT, PHIGTRON, CARM, Peniotron, etc.

Coaxial Cavity Gyrotron (Group 4)

Coaxial insert (central conductor) close to the electron beam solves the problem of voltage depression and corresponding degradation of electronic efficiency

Coaxial insert increases the space-charge limiting current and hence allows for large beam current

Down tapered central conductor makes the ratio of the outer radius to the inner radius of the cavity (taper parameter) increase toward the output end

Structure parameters are so designed as to make the slope of the eigenvalue versus taper parameter characteristics more positive for the mode of interest than for the competing modes

As the wave propagates towards the output end, the mode of interest moves more towards the lower cutoff frequencies and hence towards lower group velocities than the competing modes. This makes the diffractive quality factor higher and hence the start-oscillation current lower for the mode of interest than for the competing modes, and hence reduces the mode competition

Mode rarefaction can be made more effective by corrugating the central conductor by azimuthally periodic axial slots and optimising the corrugation geometry

Vane-loaded Gyrotron (Group 4)

Vanes create a periodic fringe field near the axis-circling electrons thus enriching the harmonic contents of RF fields as experienced by the electrons. By adjusting the depth of the vanes one can position the fringe fields around electrons moving in small orbits of small Larmor radii in the large-orbit configuration

High harmonic operation for reduced required magnetic field
Low energy beam owing to small-diameter axis circling beam
Good mode selectivity

Quasi-Optical Gyrotron (QOG) (Group 4)

Separates the functions of beam collection and microwave output coupling
RF waves are excited in an open two-mirror resonator, and a suitable waveguide system is provided for transporting power to the desired location

In a version of QOG, the electron beam is parallel to the cavity mirrors capitalising on the feature that at the near-cutoff frequency of a gyrotron, the flow of microwave power in the cavity is largely perpendicular to the electron beam

The device has ability to spread radiation beam out on a large reflecting mirror. Distancing the structure walls from the microwave interaction region reduces power losses in the open-resonator system, making the device of relevance to high-average power applications such as fusion plasma heating

A mode converter is done away with in the device, since it can couple radiation out of the cavity directly in a Gaussian mode

The device has a provision for mechanical tuning of the operating frequency by changing the distance between mirrors

Large-Orbit Gyrotrons (LOG) (Group 4)

Cusp gun provides waveguide-axis-encircling beam orbits.

Requires less background magnetic field as it can be operated at high beam harmonics [$\omega_c = \omega / s$].

A typical large-orbit gyrotron has delivered 600 MW of output power at the 20th cyclotron harmonic (s =20).

Typical Gyrotron Output Specifications

Conventional gyrotrons:
Pulsed power: 340 kW in the ka-band; 1.1 MW at 100 GHz and 645 kW at 140 GHz; CW power: 200 kW at 28-60 GHz; 100 kW at 140 GHz.. Short-pulse gyrotrons (<10 ms): 2.1 MW output at 100 GHz, 30% efficiency; 1.2 MW at 231 GHz, 20% efficiency.
Long-pulse or quasi-CW gyrotrons: 1.05 MW output at 8 GHz; 0.37 MW at 110 GHz; 10 kW at 503 GHz, 5.5% efficiency (pulse length: 0.0015 ms).

Relativistic gyrotrons: (beam voltage: 3.3 MV, beam current: 80 kA); 1000 MW at 8.35-13 GHz, 0.4% efficiency.

Coaxial cavity gyrotron (operating in the $TE_{20,13}$ mode, in which the inner conductor was down tapered towards the output end): 2.1 Mw of power at 100 GHz.

QOG: 1 kW CW at 34 GHz (9 %frequency tunability); 600 kW (pulse length: 0.013 ms) at 120 GHz, 9% efficiency.

Commercial gyrotrons: 200 kW at 60 GHz and 100 kW at 140 GHz.

Gyro-TWT, CARM, and SWCA

Beam-mode dispersion relation

$$\omega - \beta v_z - s\omega_c / \gamma = 0$$ s is the beam harmonic number

$$\omega = \beta v_z + s\omega_c / \gamma = \omega_D$$ Doppler-shifted cyclotron angular frequency

$$\Delta\omega_D = \beta \Delta v_z - \frac{s\omega_c}{\gamma^2}\Delta\gamma$$

Δv_z caused by Weibel instability due to Lorentz force on electrons in transverse motion in transverse RF magnetic field

$$\gamma m \frac{dv_z}{dt}\vec{a}_z = e(\vec{v}_\perp \times \vec{B}_\perp)$$

With the help of Maxwell equations and a vector identity

$$\Delta v_z = \frac{e}{\gamma m}\frac{\beta}{\omega}(\vec{v}_\perp . \vec{E}_\perp)\Delta t$$ (Weibel instability term)

$$\Delta v_z = \frac{e}{\gamma m}\frac{\beta}{\omega}(\vec{v}_\perp . \vec{E}_\perp)\Delta t$$ (Weibel instability term)

$\Delta\gamma$ caused by energy exchange between electrons with transverse motion in transverse RF electric field

$$\frac{d}{dt}(\gamma mc^2) = e(\vec{v}_\perp \cdot . \vec{E}_\perp)$$

$$\Delta\gamma = \frac{e}{mc^2}\frac{\beta}{\omega}(\vec{v}_\perp . \vec{E}_\perp)\Delta t$$ (CRM instability term)

$$\Delta\omega_D = \beta\,\Delta v_z - \frac{s\,\omega_c}{\gamma^2}\Delta\gamma$$

Two terms in $\Delta\omega_D$ tend to cancel each other, pointing towards auto-resonance.

Substituting Δv_z and $\Delta\gamma$

$$\Delta\omega_D = \beta\,\Delta v_z - \frac{s\,\omega_c}{\gamma^2}\Delta\gamma$$

$$= \frac{e}{m}\left[\frac{\beta^2}{\omega\gamma} - \frac{s\omega_c}{\gamma^2 c^2}\right](\vec{v}_\perp . \vec{E}_\perp)\Delta t$$

Auto-resonance condition $\Delta\omega_D = 0$ leads to

$\frac{\beta^2}{\omega\gamma} - \frac{s\omega_c}{\gamma^2 c^2} = 0$ Weibel and CRM instabilities are present in equal proportions

In view of $\frac{s\omega_c}{\gamma} \lesssim \omega$, the above condition in turn leads to

$\frac{\omega}{\beta} \gtrsim c$ Corresponds to destabilisation of mildly fast waveguide mode in a cyclotron auto-resonance maser (CARM)

$\frac{\beta^2}{\omega\gamma} > \frac{s\omega_c}{\gamma^2 c^2} \Rightarrow \frac{\omega}{\beta} < c$ Weibel instability dominates — slow-wave destabilisation: slow-wave cyclotron amplifier (SWCA)

$\frac{s\omega_c}{\gamma^2 c^2} > \frac{\beta^2}{\omega\gamma} \Rightarrow \frac{\omega}{\beta} > c$ CRM instability dominates — fast wave destabilisation : gyro-TWT

Gyro-TWT (Group 4)

Gyro-TWT operates at grazing intersection between the beam-mode and waveguide-mode dispersion characteristics

At the operating point, the slope of the beam-mode dispersion line and the slope of the tangent to the waveguide-mode dispersion hyperbola become equal: $v_z = v_g$

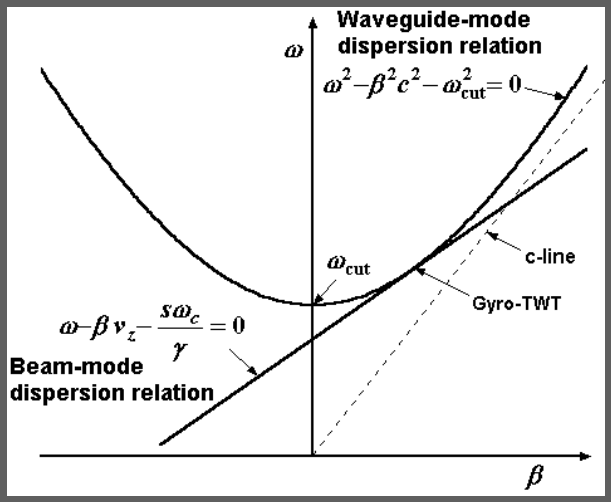

Gyro-TWT operating point

$$\frac{\omega}{\beta} > c$$

CRM instability dominates to destabilise fast wave waveguide mode

Bunching in a Gyro-TWT

Axial phase synchronism between the electrons gyrating in helical paths and a co-propagating travelling RF wave supported by the waveguide

Electrons moving in helical paths form into a bunch that twists around the helix system with a pitch substantially greater than the electron pitch.

Spatial position, where electrons in the bunch are decelerated, advances with a phase velocity approximately equal to the phase velocity of the waveguide

- A continuous interaction and energy transfer takes place from the phase-modulated electrons to the RF wave over a relatively long interaction length

Usually operated at frequencies between the cutoff and the grazing points

- As the axial wavenumber grows, the operation of a gyro-TWT becomes more sensitive to electron velocity spread

A number of stages with severs to be provided for stability with large gains

Conditions for grazing intersection or coalescence between the beam-mode and waveguide-mode dispersion characteristics

Dispersion relation for cyclotron wave

$$\omega - \beta v_0 \mp \omega_c = 0$$ (upper sign for the fast cyclotron wave)

Dispersion relation for fast cyclotron wave: $\omega - \beta v_0 - \omega_c = 0$

Beam-mode dispersion relation: $\omega - \beta v_z - \frac{s\omega_c}{\gamma} = 0$

(for beam harmonic s operation)

$$\gamma = (1 - \frac{v_z^{\,2} + v_t^{\,2}}{c^2})^{-1/2}$$

$$\gamma = 1 + \frac{|e|V_0}{mc^2}$$

Beam-mode dispersion relation: $\omega - \beta v_z - \frac{s\omega_c}{\gamma} = 0$ $\left[\omega_c = \frac{|e|B}{m}\right]$

Waveguide-mode dispersion relation: $\omega^2 - \beta^2 c^2 - \omega_{cut}^2 = 0$

$$2\omega\frac{\partial\omega}{\partial\beta} - 2\beta c^2 = 0 \quad \Rightarrow \quad \frac{\partial\omega}{\partial\beta} = \frac{\beta c^2}{\omega} \quad \Rightarrow \quad v_g = \frac{\partial\omega}{\partial\beta} = \frac{\beta c^2}{\omega}$$

Grazing intersection: $v_z = v_g \quad \Rightarrow \quad v_z = \frac{\beta c^2}{\omega}$

From $\omega - \beta v_z - \frac{s\omega_c}{\gamma} = 0$ and $v_z = \frac{\beta c^2}{\omega} \quad \Rightarrow \quad \omega = \frac{s\omega_c}{\gamma}\gamma_z^{\,2}$ $\left[\gamma_z = (1 - \frac{v_z^{\,2}}{c^2})^{-1/2}\right]$

From $\omega^2 - \beta^2 c^2 - \omega_{cut}^2 = 0$ and $v_z = \frac{\beta c^2}{\omega} \quad \Rightarrow \quad \omega = \omega_{cut}\gamma_z$

$$\omega = \frac{s\omega_c}{\gamma}\gamma_z^{\,2} = \omega_{cut}\gamma_z \quad \Rightarrow \text{ Grazing magnetic flux density } B = \frac{\gamma}{\gamma_z}\frac{m}{|e|}\frac{1}{s}\omega_{cut}$$

•Features of conventional TWT and gyro-TWT

Conventional TWT

- Cerenkov radiation type
- Magnetic field for beam confinement
- Larger magnetic field at higher frequencies for beam confinement
- Conversion of axial beam kinetic energy
- Axial non-relativistic electron bunching
- Near-synchronism between DC beam velocity and circuit phase velocity

Gyro-TWT

- Bremsstrahlung radiation type
- Magnetic field for beam-wave interaction
- Larger magnetic field at higher frequencies for cyclotron resonance
- Conversion of azimuthal beam kinetic energy
- Azimuthal relativistic electron bunching
- Near-synchronism between wave frequency and cyclotron frequency

(*Continued*)

Conventional TWT

- Electron beam velocity to be slightly greater than RF phase velocity
- Slow space-charge wave on electron beam to couple to forward circuit wave
- Space-charge-limited operation
- Pierce gun
- Smaller structure sizes at higher frequencies

Gyro-TWT

- Wave frequency to be slightly greater than cyclotron frequency
- Fast cyclotron wave on electron beam to couple to forward waveguide mode
- Temperature-limited operation
- MIG
- Relatively larger structure sizes at higher frequencies

Harmonic multiplying gyro-TWT (Group 4)

Two-stage nonlinear device (electron pre-bunched for a better harmonic content)

Less magnetic field required due to beam harmonic (cyclotron harmonic) operation

Less expensive input drive required due to low-frequency input

First stage operates at the fundamental frequency ω_1

Second stage operates at a chosen harmonic (q) frequency $\omega_2 = q\omega_1$

Magnetic field same in both the stages: $\omega_{c1} = \omega_{c2}$

Beam harmonic mode number of the second stage (s_2) is the 'chosen frequency harmonic' (q) times the beam harmonic mode number of the first stage (s_1): $s_2 = qs_1$

[$\omega_2 = q\omega_1$; q is the harmonic multiplying number]

$\omega_{c1} = \dfrac{\omega_1}{s_1}$ and $\omega_{c2} = \dfrac{\omega_2}{s_2}$ [s_1 and s_2 are the beam harmonic numbers]

$\omega_{c1} = \omega_{c2}$ (same magnetic field in the two stages)

leading to $\omega_2 = q\omega_1$]

PHIGTRON (Group 4)

Harmonic multiplying inverted gyro-twystron

Twystron: First stage: input cavity (klystron)
Second stage: output waveguide (TWT)

✓Inverted twystron: First stage: input waveguide (TWT)
Second stage: output cavity (klystron)

UMD developed Ku-to-Ka band (16.85-to-33.7 GHz) PHIGTRON driven by 2 kW Ku-band helix TWT:

Typical output parameters:
Higher power: 720 kW, 34% efficiency, 33 dB, 0.3% bandwidth
Wider bandwidth: 400 kW, 35% efficiency, 30 dB, 0.7% bandwidth

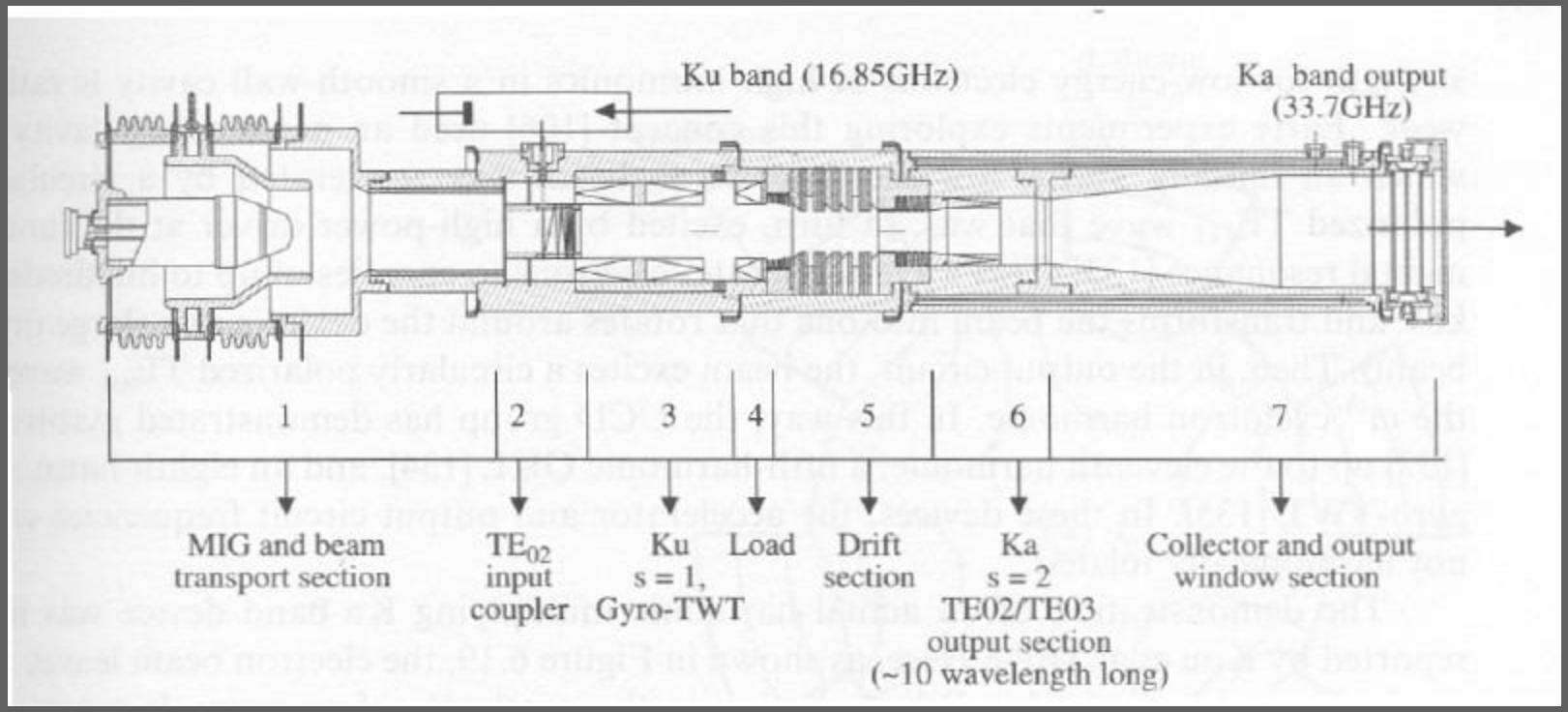

Phigtron schematic

CARM (Group 4)

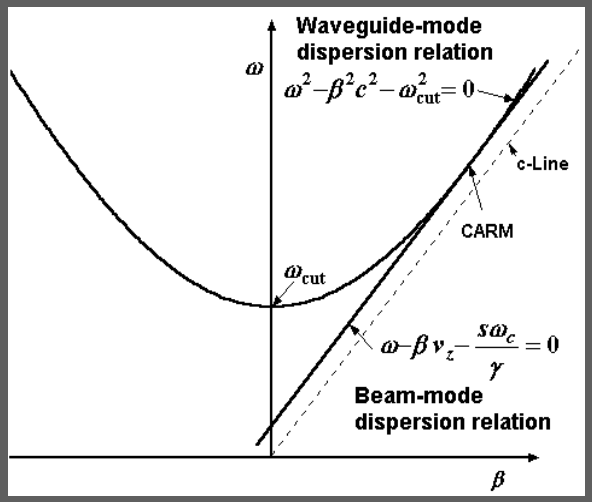

CARM operating point

Weibel and CRM instabilities are simultaneously present in equal proportions balancing the effects due to each other leading to auto-resonance.

Once the electron beam is phase-bunched, a large amount of energy could be extracted without loosing synchronism (auto-resonance).

Mildly fast waveguide mode destabilized $\omega/\beta \gtrsim c$

Requires lesser magnetic field due to a large Doppler shift $v_z \ \beta$

$$s\omega_c/\gamma = \omega - \beta v_z$$

(beam-mode dispersion relation)

Operated far from cutoff at a large value of the axial phase propagation constant β and hence sensitive to beam velocity spread causing inhomogeneous broadening of the cyclotron resonance band

Operates at a lower beam pitch factor, higher beam voltage, with higher power capability, and at higher frequencies

Higher efficiency, since the axial kinetic energy is tapped

Increased stability due to higher axial electron velocities

Reduced gain caused by axial bunching offsetting azimuthal bunching

Wider device bandwidth due to wideband coalescence between the the beam-mode and waveguide-mode dispersion characteristics

Typical CARM Performance

10 MW, 35 GHz, 45 dB gain and 3% efficiency (1.5 MV, 0.25 kA)
10 MW at 125 GHz, 2% efficiency (0.5 MV, 1.0 kA)

Gyro-BWO (Group 4)

Frequency tunable over a wide (octave) range by changing the beam voltage or magnetic field

Constant output (within 3 dB) over a wide range of frequencies

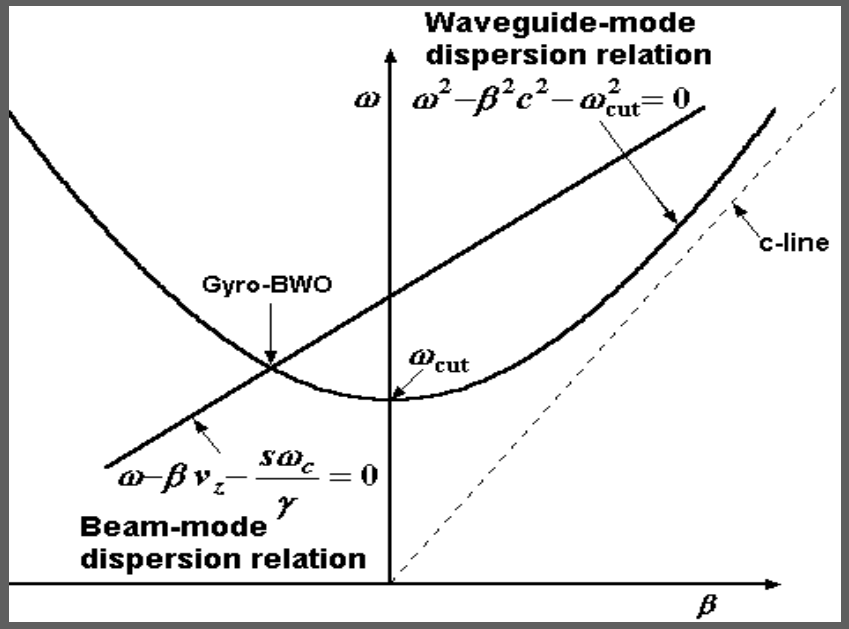

Gyro-BWO operating point

Problem areas:

$$\omega - \beta v_z - s\omega_c / \gamma = 0 \quad \text{(beam-mode dispersion relation)}$$

to be read as $s\omega_c / \gamma = \omega - \beta v_z = \omega + |\beta| v_z$ (negative β)

Larger magnetic field is required in a gyro-BWO than in a gyrotron

Gyro-BWO features *continued*

When magnetic field is changed for tuning, the beam position to experience maximum RF electric field changes, and also mode completion increases.

The field of a large-amplitude wave modulates the electrons entering the interaction region; while the deceleration of the electron bunches occur in the region of small-amplitude wave, resulting in the degradation of efficiency.

In a typical gyro-BWO, the power is extracted near the cathode by a bevel-cut rectangular waveguide:

Tunable over 4.2-5.2 GHz, 100-180 kW; 150-600 ns (TE_{01}); 4 MW, 80 ns (TE_{21}).

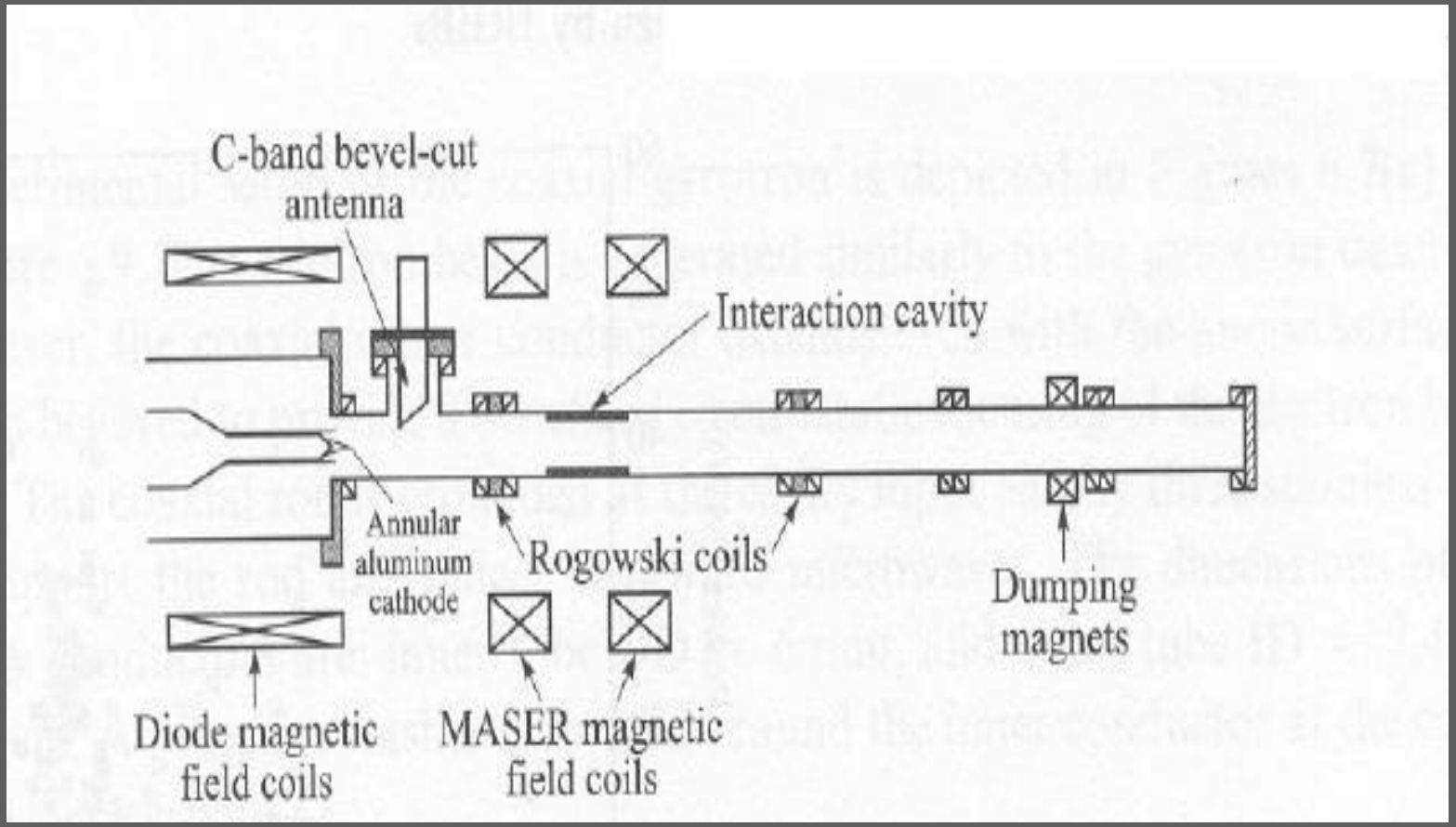
C-band bevel-cut antenna
Interaction cavity
Annular aluminum cathode
Rogowski coils
Dumping magnets
Diode magnetic field coils
MASER magnetic field coils

Gyro-BWO

Thank you!

Appendix

Peniotron (Group 4)

High efficiency fast-wave gyro-device even at high beam harmonic modes

No relativistic azimuthal bunching — a selection mechanism

Both initially accelerated and initially decelerated electrons deliver energy to RF waves

The orbital radius of an initially accelerated electron increases after half rotation
The orbital radius of an initially decelerated electron decreases after half rotation
The drift of the guiding center of the orbiting electrons occurs in such a way that the electrons move into a stronger electric field region during their decelerating phase, whereas they move into a weaker electric field region during their accelerating phase. As a result all electrons, when averaged over one orbit period, lose practically the same energy irrespective of their initial phase distribution when averaged over one orbit period.

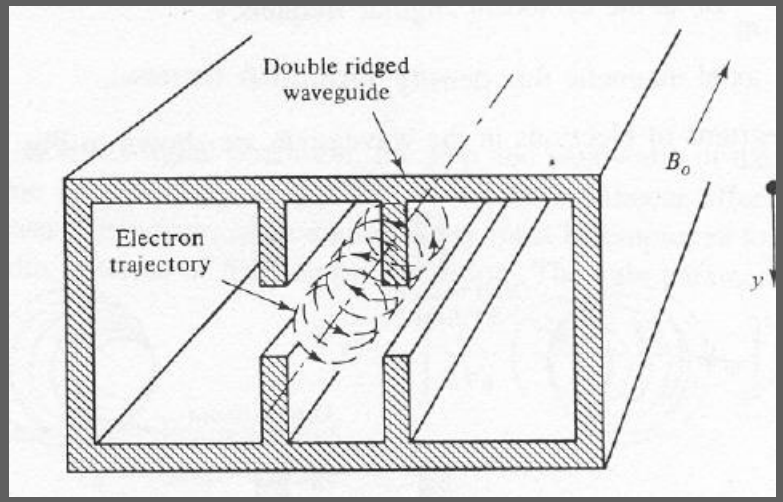
Double ridged
waveguide
Electron
trajectory
B_o
y

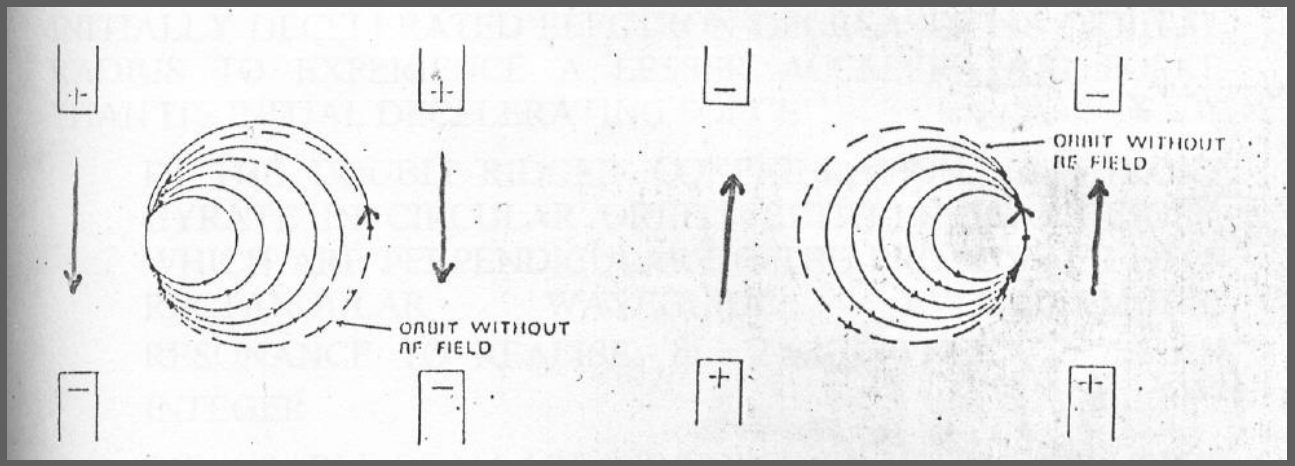
ORBIT WITHOUT
RF FIELD
ORBIT WITHOUT
RF FIELD

Initially accelerated electron is decelerated after half rotation, if the field changes by a cycle or a number of cycles

Initially accelerated electron is decelerated after half a rotation, if the field reverses its phase

Initially accelerated electron is accelerated after half a rotation, If the field changes by a cycle or a number of cycles

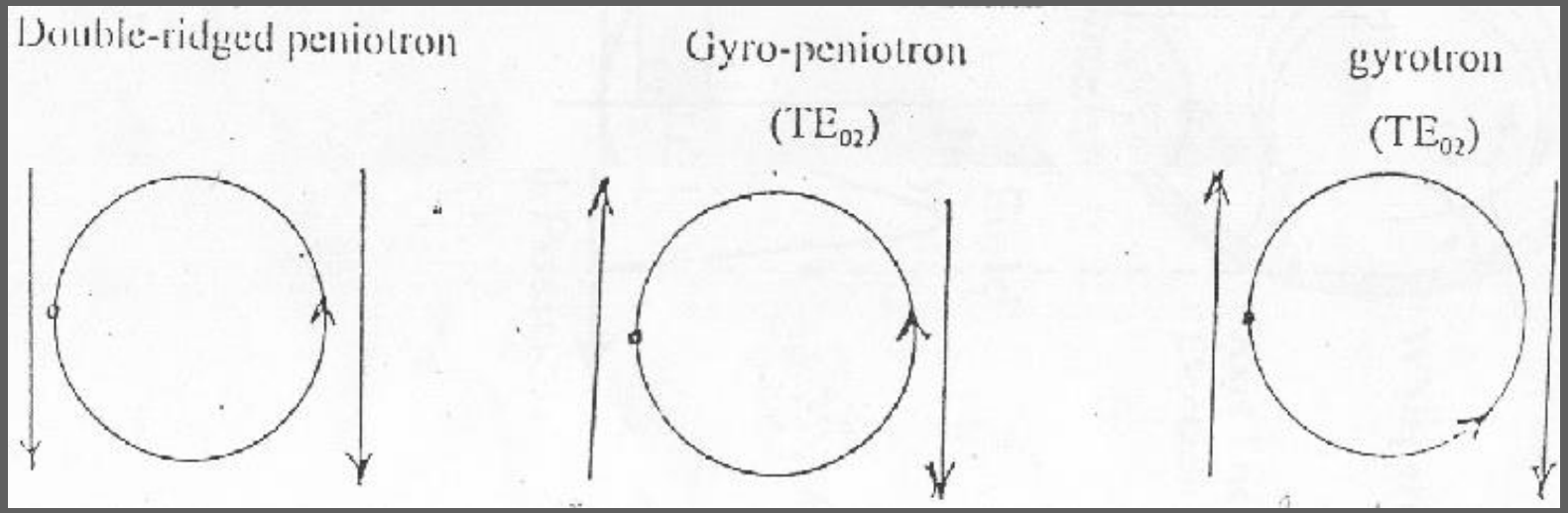

$$\frac{T_c}{2} = T,\ 2T,\ 3T,.... = pT$$

$$T_c = 2pT$$

$$\omega = 2p\omega_c$$

Even cyclotron harmonic resonance

$$\frac{T_c}{2} = \frac{T}{2},\ \frac{3T}{2},.... = \frac{(2p-1)}{2}T$$

$$T_c = (2p-1)T$$

$$\omega = (2p-1)\omega_c$$

Odd cyclotron harmonic resonance

$$\frac{T_c}{2} = T,\ 2T,\ 3T,.... = pT$$

$$T_c = 2pT$$

$$\omega = 2p\omega_c$$

Even cyclotron harmonic resonance

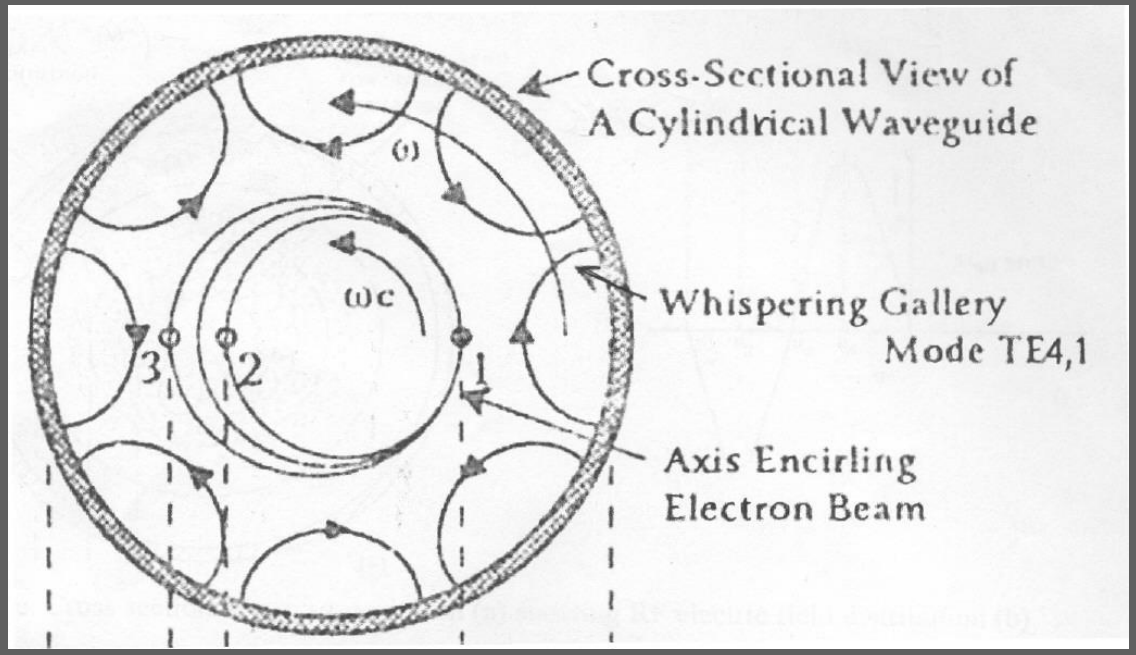

$T_c/2 = T/2,\ 3T/2,\ 5T/2,\ \ldots$

$T_c = 3T$

$\omega = 3\omega_c$

$\omega = s\omega_c$

$m = 4$

$\omega - \beta v_z - s\omega_c = 0$

$\omega = s\omega_c$

Here $s = 3 = 4 - 1$

In general $s = m - 1$

For a peniotron $\omega - \beta v_z - (m-1)\omega_c = 0$

For a gyro-peniotron, the beam-mode harmonic number s is related to the azimuthal waveguide mode number as $s = m - 1$

Beam-mode dispersion relation to be read as: $\omega - \beta v_z - (m-1)\omega_c = 0$

(non-relativistic)

Output parameters: 10 GHz, 10 kW (pulsed), $TE_{1\,1}$ rectangular, 36% efficiency

Vane-loaded (magnetron-like structure) peniotron:

$TE_{4\,1}$ whispering-gallery mode, 8 vanes, 20 kW

3rd beam harmonic, 70% efficiency (Tohoku University)

There is a proposal to build a 40 MW gyro-peniotron at 200 GHz using an auto-resonance amplifier configuration

Photonic Bandgap (PBG) Structure

PBG structure (with lattice defect) proposed by Yablonovitch to suppress spontaneous emission in semiconductors

A triangular lattice of metal rods parallel to the axis of the gyrotron and magnetic field system replaces the cylindrical wall of the waveguide resonator

A number of rods are removed from the center of the array to form a ‘defect’ to support a defect mode in the bandgap

The bandgap is adjusted such that the frequencies of all other neighbouring modes lay in the propagating band of the lattice and hence they leak through the array and could be absorbed at the periphery of the array

Thus, the PBG structure gives single-mode performance (typically TE_{041}-mode gyrotron and TM_{010}-mode linear accelerator)

Specifications of gyro-TWTs developed in some typical laboratories

(*Compiled by Vishal Kesari* <vishal_kesari@rediffmail.com>)

Operating frequency (GHz) / band	Power (kW)	Efficiency (%)	Gain (dB)	Bandwidth (%)/ 3-dB Bandwidth (GHz)	Mode/ Loading/ Tapering	Reference Year
35	340	51	2 (per cm)	2.6	Circular TE_{01}	Chu *et al.* 1979
35	100	>10	17	~ 10	—	Seftor *et al.* 1979
35	—	—	24	1.4	—	Barnett *et al.* 1979
35.1	—	—	32	—		
35	26	—	13	—		
35	10	—	30	—		
35		7.8	20	—		
35.12	3.2	—	42	—	Circular TE_{01} Resistive wall loading	Barnett *et al.* 1980
35.5	—	—	26 (Peak)	3.4		
~ 35	—	—	34	2		
5.2	50	16.6	—	6	Circular TE_{11} Non-tapered magnetic field	Ferguson *et al.* 1981
5.2	128	24	20	7.25	Circular TE_{11} Tapered magnetic field	
	18.8	9.8		9.3		
94	28	8	30	8	Circular TE_{11}	Eckstein *et al.* 1981

[*Continued*]

[*In continuation*]

Specifications of gyro-TWTs developed in some typical laboratories

(*Compiled by Vishal Kesari* <vishal_kesari@rediffmail.com>)

Operating frequency (GHz) / band	Power (kW)	Efficiency (%)	Gain (dB)	Bandwidth (%)/ 3-dB Bandwidth (GHz)	Mode/ Loading/ Tapering	Reference Year
35	—	—	18	13	Circular TE_{01} Tapered cross section and magnetic field	Barnett *et al.* 1981
94	20	8	30	2	—	Granastein and Park 1983
—	—	25	45	45	Two-stage tapered cross section	Ganguly and Ahn 1984
35	20×10^3	11	30	—	—	Gold *et al.* 1989
Ku-band	18.4	18.6	18	10	—	Chu *et al.* 1990
Ka band	27 (Peak)	16	35	7.5	Circular TE_{11}	Chu *et al.* 1990
35	5	10 (Saturated)	20	33	Rectangular TE_{10} Tapered cross section and magnetic field	Park *et al.* 1991
9-11	80	30 (Saturated)	15	20	Rectangular Dielectric loaded	Leou *et al.* 1992

[*Continued*]

[*In continuation*]

Specifications of gyro-TWTs developed in some typical laboratories

(*Compiled by Vishal Kesari* <vishal_kesari@rediffmail.com>)

Operating frequency (GHz) / band	Power (kW)	Efficiency (%)	Gain (dB)	Bandwidth (%)/ 3-dB Bandwidth (GHz)	Mode/ Loading/ Tapering	Reference Year
35	533	21.3	20	7.4	Circular TE_{21} Three-stage	Wang *et al.* 1992
35	7.4	15	30	8	—	Park *et al.* 1993
Ka-band (27-38 GHz)	—	10 (Saturated)	25	33	Two-stage	Park *et al.* 1994
35	8 (Saturated)	16	25	20	Two-stage Tapered	Park *et al.* 1995
34.2	62	21	33	12	—	Chu *et al.* 1995
Ku-band	207	12.9	16	2.1	—	Wang *et al.* 1995
16.7	207	—	—	—	Circular TE_{21} Axially sliced	Wang *et al.* 1996
15.9	20	—	—	—	Dielectric loaded	Wang *et al.* 1996
X-band	55	11	27 (Saturated)	11 (Constant) > 14 (Saturated)	Rectangular TE_{10} Dielectric loaded	Leou *et al.* 1996

[*Continued*]

[*In continuation*]

Specifications of gyro-TWTs developed in some typical laboratories

(*Compiled by Vishal Kesari* <vishal_kesari@rediffmail.com>)

Operating frequency (GHz) / band	Power (kW)	Efficiency (%)	Gain (dB)	Bandwidth (%)/ 3-dB Bandwidth (GHz)	Mode/ Loading/ Tapering	Reference Year
Ka-band	—	—	50 (Saturated)	—	—	Chu *et al.* 1997
X-band	55- 75	—	30	20	Rectangular Metal disc-loaded	Leou *et al.* 1998
95	6	5	11	3	Slotted structure	Chong *et al.* 1998
Ka band	93 (Saturated peak)	26.5	70	3 GHz (3-dB)	Lossy section	Chu *et al.* 1998
X-band	1×10^3	20	23	—	Helical waveguide	Denisov *et al.* 1998
—	—	28	38	19	Helical waveguide	Denisov *et al.* 1998
—	—	—	29 (Peak)	10	Helical waveguide	Cooke *et al.* 1998
35	2×10^3	20	30 (Saturated)	3.5	Circular TE_{41} Sliced waveguide	McDermott *et al.* 1998
Ka-band	100	26.5	70	8.6	Circular TE_{11} Lossy graphite covered wall	Chu *et al.* 1999

[*Continued*]

[*In continuation*]

Specifications of gyro-TWTs developed in some typical laboratories

(*Compiled by Vishal Kesari* <vishal_kesari@rediffmail.com>)

Operating frequency (GHz) / band	Power (kW)	Efficiency (%)	Gain (dB)	Bandwidth (%)/ 3-dB Bandwidth (GHz)	Mode/ Loading/ Tapering	Reference Year
35	93 (Saturated)	26.5	70	8.6	Circular TE_{11}	Chu *et al.* 1999
9.2	1.1×10^3	29	37 (Saturated) 47 (Linear)	21	Helically waveguide	Bratman *et al.* 2000
91.4	600	24	30	2.7	Circular TE_{02}	Wang *et al.* 2000
92	140	28	50 (Saturated)	5	Circular TE_{01} Distributed-loss circuit	McDermott *et al.* 2001
35	137 (Saturated)	17	47	3.3	Circular TE_{01} Ceramic rings (distributed attenuation)	Garven *et al.* 2002
32.9	155	15	45	2.2 GHz (3-dB)	Multistage	Yeh *et al.* 2003
140	30 (Peak)	12	29	2.3 GHz (3-dB)	Confocal waveguide HE_{06}	Sirigiri *et al.* 2003
34.2	—	10	23.8	4.1	Rectangular Two-stage tapered	Baik *et al.* 2003

[*Continued*]

[*In continuation*]

Specifications of gyro-TWTs developed in some typical laboratories

(*Compiled by Vishal Kesari* <vishal_kesari@rediffmail.com>)

Operating frequency (GHz) / band	Power (kW)	Efficiency (%)	Gain (dB)	Bandwidth (%)/ 3-dB Bandwidth (GHz)	Mode/ Loading/ Tapering	Reference Year
34.2	—	12	23.8	4.1	Rectangular Two-stage tapered	Baik *et al.* 2003
—	—	53	—	27	Coaxial irregular waveguide TE_{01}	Kolosov *et al.* 2003
Ka-band	20	—	—	—	Two-stage tapered (Frequency multiplication)	Baik *et al.* 2004
Ka-band	>3 kW	—	< 20 dB/m	4	Two-stage tapered (Frequency multiplication)	Baik *et al.* 2004
Ka-band	435	31	45	~ 5.8	Coaxial waveguide	Hung and Yeh 2005
W-band	≥ 0.5	—	≥ 45	≥ 8 GHz (3-dB)	Circular TE_{01}	Blank *et al.* 2005
95	15	6.2	30	1.6	—	Granastein and Alexeff
95	28	8	31 (Saturated)	—	—	CPI (Varian)
Ka-band	52		60	12	Circular TE_{11} Diffractive loading	Pershing *et al.*
	70		60	17		